(5′-TGCACTTTAGGATCCCCCATTAGTCCTA-3′), 66R (5′-ATCTA TTCCAAGCTTTTATAGTACTTTCCT-3′), and 51R (5′-GGCTG CCCCAAGCTTTTAGAAAGTTTCTGC-3′) (underlines denote *Bam*HI and *Hin*dIII recognition sites) were used to produce fragment DNAs by polymerase chain reaction (PCR) using pNL43 [10]. The primers 66F/66R were used for P66 cDNA (2550–4229) and 66F/51R for P51 cDNA (2550–3869). Each PCR fragment was subcloned into the bacterial expression vector pQE-9 (Qiagen) at the downstream region of the His_6-tag sequence between *Bam*HI and *Hin*dIII sites, and transformed in XL-1 Blue (Strategene). *Escherichia coli* pellets containing P66 and P51 were suspended in the buffer containing 20 mM sodium phosphate (pH 7.0), 50 mM NaCl, and a protease inhibitor cocktail without EDTA (Roche) following a double pass through a French press at approximately 1.5 kgf/cm^2. The samples were ultracentrifuged in an SW41 rotor at 25,000*g* for 30 min at 4 °C and the supernatants were applied to an HiTrap chelating column (Amersham–Pharmacia). The concentration of NaCl was adjusted to 50 mM in imidazole-eluted fractions and the fractions were applied to a (1.0 × 2.0 cm) Hitrap SP column (Amersham–Pharmacia) equilibrated with 20 mM sodium phosphate (pH 7.0) and 50 mM NaCl. The RT protein was eluted from the column using a linear gradient of NaCl at concentrations ranging from 0.05 to 0.4 M (total volume 18 ml). The purity of purified proteins was 90% as determined by Coomassie brilliant blue staining of the sodium dodecyl sulfate (SDS)–polyacrylamide gels. The peak fractions were mixed with 20 mM sodium phosphate (pH 7.0), 1 mM dithiothreitol (DTT), 0.1 M NaCl, and 50% glycerol. Expression and purification of GST-gag proteins was previously described [5,8]. Murine leukemia virus RT was purchased from Roche Diagnostics.

Human topoisomerase I cDNA was amplified by PCR, using the primers, TF (5′-CGT CCC TCC GAA TTC ATG AGT GGG GAC CA-3′) and TR (5′-GCC TCT TGA GCG GCC GCT AAA ACT CAT AGT CA-3′) (underlined sequences correspond to *Eco*RI and *Not*I recognition sites, respectively). Wild type (wt) human topoisomerase I cDNAs were subcloned into baculovirus transfer vectors with six His-tag-sequences at the N-terminus (pFASTBAC HTa, Invitrogen). Recombinant baculovirus was prepared according to the manufacturer's instructions. The nuclei of infected insect cells were resuspended with phosphate buffer [20 mM phosphate (pH 7.5), 1 M NaCl, 10 mM imidazole, and 1 tablet of protease inhibitor cocktail without EDTA (Roche)]. Following precipitation of polynucleotides with 6% polyethylene glycol 6000, supernatants were applied to HiTrap chelating columns. Imidazole-eluted fractions were applied to 1.0 ml UNO S-1 (Bio-Rad), cation exchange columns. Wt topoisomerase I was eluted from the column by a high concentration of NaCl and separated by SDS–polyacrylamide gel electrophoresis (PAGE). After staining with SYPRO (Molecular Probes), the polyacrylamide gel was visualized with FLA 2000 (Fuji film).

Synthesis of SL1 RNA. To analyze the binding of HIV-1 RT and topoisomerase I to structured RNAs, we used a stem loop RNA (SL1) (59 nt) derived from HIV-1 dimer initiation site (DIS) and longer RNAs (180 nt) from plasmids. SL1F (5′-TAATACGACTCACTATAGGGAGATCTCTCGACGCAGGACT-3′) and SL1R (5′-CCCCTCGCCTCTTGCCGTGCGCGCTT-3′) were used to synthesize SL1 RNA (corresponding to 677–734 nt of pNL43) as previously described [11]. Two 180 mer RNAs containing 100 nucleotides (nt) of complementary regions (Fig. 1D) were transcribed from pSP72 and pSP73 (Promega) by T7 RNA polymerase (Ambion). RNA from pSP72 was internally labeled with [α-^{32}P]CTP. Both RNAs were hybridized in 50 mM Tris–HCl (pH 8.0) and 0.2 M NaCl, and the hybridized RNA or single-stranded RNA was purified from 6% TBE (90 mM Tris-borate, 2.5 mM EDTA) acrylamide gel.

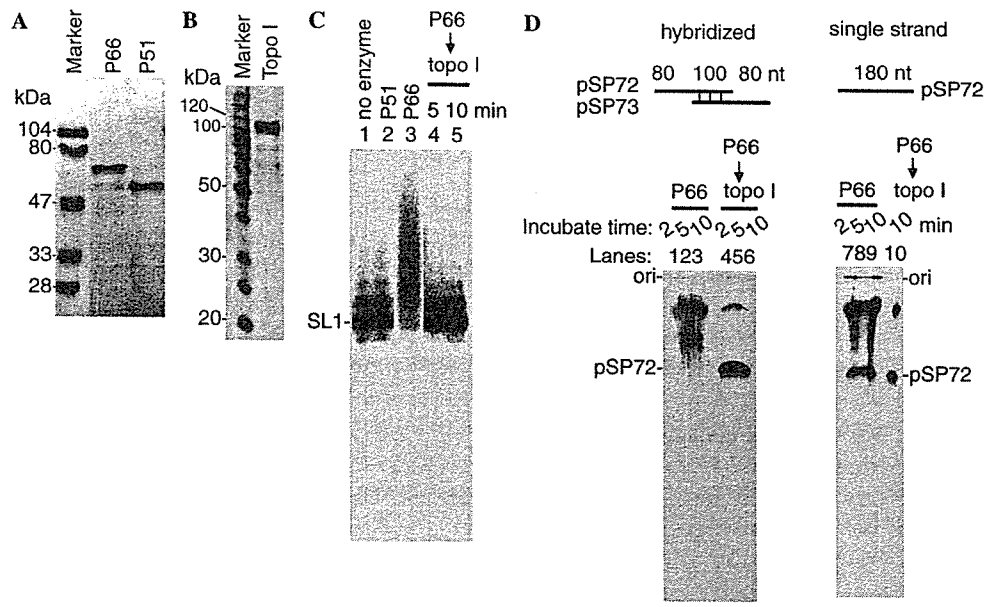

Fig. 1. Analysis of the interaction of HIV-1 RT and RNAs, and the dissociation effect of topoisomerase I to RT from the RT–RNA complex. (A,B) Electrophoresis of purified HIV-1 RT subunits, P66 and P51 (A) or human topoisomerase I (Topo I, B). The purified proteins were analyzed by SDS–PAGE and visualized by Coomassie brilliant blue staining (A) or SYPRO staining (B). The molecular size markers are indicated on the left side. (C) Electrophoresis of RT and [α-^{32}P]CTP-labeled SL1 RNA mixture samples in the presence and absence of topoisomerase I. Binding reaction mixtures containing only SL1 RNA substrates (lane 1), and additionally including P51 (lane 2) or p66 (lane 3) were incubated for 10 min at 37 °C. Samples were further incubated with topoisomerase I for 5 min (lane 4) or 10 min (lane 5). After incubation the reactions were extracted by phenol and chloroform treatment, precipitated with ethanol, and dissolved in water. Heated samples were loaded on a denaturing acrylamide gel. (D) Similar binding reactions as (C) except using longer substrates (partially double-stranded RNA composed of a 100-bp double-stranded region and an 80-mer single-stranded region or a 180-mer single-stranded RNA). The samples were incubated with P66 in the absence of topoisomerase I for 2, 5 or 10 min (lanes 1, 2, 3, 7, 8, and 9), or incubated with P66 for 5 min following incubation with topoisomerase I for 2, 5 or 10 min (lanes 4–6), or for 10 min (lane 10).

Binding and dissociation of P66 proteins. For the analysis of RT binding to RNAs, reaction mixtures (20 μl) containing 50 mM Tris–HCl (pH 8.0), 50 mM NaCl, 5 mM $MgCl_2$, 4 mM DTT, 10 ng of internally labeled substrates, and 20 ng P66, P51 were incubated at 37 °C. For the dissociation by topoisomerase I, mixtures (20 μl) containing 50 mM Tris–HCl (pH 8.0), 50 mM NaCl, 5 mM $MgCl_2$, 10 μl of the binding reaction products, and 50 ng of topoisomerase I were allowed to react for the indicated times at 37 °C. Formamide was added to the samples for a final concentration of 20% and the samples were heated for 4 min at 85 °C. Reaction products were then analyzed by electrophoresis on 6–12% polyacrylamide sequence gels containing 7 M urea in TBE. Following electrophoresis, the gels were dried for phosphorimage analysis (FLA2000, Fuji Film).

The experiments of binding and dissociation of P66 proteins were performed on a BIAcore 3000 biosensor (Biacore). All experiments were performed at 25 °C using a Hepes buffer (pH 7.4) with 20 mM NaCl and 5 mM $MgCl_2$. The buffer flow was 2 μl/min. Sensor chip SA (Biacore) was pre-coated with streptavidin. The 3′-biotinylated oligonucleotide (5′-AAATGCGTCGAGAGATCTCC AAAAAA-3′) and SL1 RNA were prehybridized in solution (25 mM Tris–HCl, pH 8.0, 0.2 M NaCl). Sixteen to thirty microliters of the hybridized substrates was injected (2 pM/μl) and captured on the streptavidin pre-coated sensor chip (SA). After binding of P66 with the SA, the captured oligonucleotide and RNA were regenerated by injection of 0.05% SDS.

Results

Topoisomerase I dissociated P66 from RNAs

It has been reported that HIV-1 RT is a hetero- and/or homo-dimer consisting of two 66 and 51 kDa polypeptides (P66 and P51, respectively) [1]. Polymerase-active sites of RT were associated with the amino terminus of both the P66 and P51, whereas its RNA hydrolysis activity was exclusively associated with the carboxyl-terminal domain of the P66 [1]. We initially examined the binding activity of P66 and P51 which were separately synthesized and purified. The SDS–PAGE analysis revealed that each recombinant protein had a clear single band around 70 and 55 kDa in size, corresponding to the expected molecular weights (Fig. 1A). Synthesized and purified wild-type (wt) human topoisomerase I was electrophoresed on SDS–containing polyacrylamide gels (Fig. 1B). The recombinant protein containing a His-tag peptide at its N-terminus had a single band on the gel around 110 kDa in size, corresponding to the expected molecular weight. After incubation of [α-^{32}P]CTP-labeled SL1 RNAs with either P66 or P51, the smear band was detected only in the lane of the SL1 RNA in the presence of P66 (lane 3 in Fig. 1C). As this smear band was not observed in the absence of recombinant protein or in the presence of P51 (lanes 1 and 2 in Fig. 1C), it seems likely that multiple P66 randomly bound with SL1 RNA. The SL1 RNA–P66 complex was not formed in the presence of 0.5% SDS, suggesting that the binding was not covalent (data not shown).

We next examined whether topoisomerase I which binds with the stem loop RNA competes with P66 for the binding to structured RNAs. After incubation of P66-bound SL1 RNA with topoisomerase I, the smear band disappeared and the SL1 RNA migrated in a similar manner as those in the absence of P66 (lanes 4 and 5 in Fig. 1C).

In order to confirm the results, we prepared longer RNAs as substrates (180 mer) composed of a 100-bp double-stranded region and an 80-mer single-stranded region or a 180-mer single-stranded RNA (Fig. 1D). We detected the smear bands of the RNAs composed of a 100-bp double-stranded region and an 80-mer single-stranded region after incubation with P66 for 2, 5, and 10 min (lanes 1–3 in Fig. 1D); however, the smear bands disappeared after incubation with topoisomerase I for 2, 5, and 10 min (lanes 4–6 in Fig. 1D), in a manner similar to the SL RNA in Fig. 1B. In contrast, when the single-stranded 180 mer RNA was incubated with P66 for 2, 5, and 10 min, the smear formation was not as intense as that of the partially double-stranded RNA, and a single band was detected (lanes 7–9 in Fig. 1D). The smear band disappeared after incubation with topoisomerase I for 10 min (lane 10 in Fig. 1D). These results suggest that P66 bound with stem-looped, partially double-stranded, and single-stranded RNAs and topoisomerase I resulted in the dissociation of P66 from these structured RNAs.

Kinetic analysis of the function of topoisomerase I to the P66–RNA complex

Next, we examined the function of topoisomerase I in the P66–RNA complex using the BIAcore system that can measure changes in surface plasmon resonance representing the changes in the mass of molecular species bound to the surface [12]. The measured differences of the mass reflected the kinetic events including association and dissociation of complexes that were composed of bound molecules and other molecules brought into contact with them in the flow cell. Initially, the 3′-biotinylated oligonucleotide which was hybridized with SL1 RNA was immobilized on a streptavidin-coated chip (Fig. 2A). The sensorgram from the biosensor analysis revealed the association of P66 to the immobilized SL1 RNA and the formation of a P66–SL1 RNA complex shown as a plateau curve (Fig. 2B). After topoisomerase I treatment, P66 was gradually dissociated from the complex and the regeneration level decreased compared to that before the treatment with topoisomerase I. To analyze the phenomenon, we separate the reaction and compared the dissociation of P66 in the absence (Fig. 2C) and the presence (Fig. 2D) of topoisomerase I. Although the condition how much RNA could be trapped to the sensor chip affected the binding and dissociation of P66, experiments repeated more than

three times showed topoisomerase I clearly enhanced the dissociation of P66.

For synthesis of DNA in the 5′–3′ direction by the polymerase, P66 recognizes the free 3′-end of DNA and/or RNA duplex. We examined whether P66 bound with SL1 RNA in the polymerase-dependent manner with the substrates hybridized with 3′- and 5′-biotinylated oligonucleotides. As both substrates demonstrated the same results (data not shown), suggesting that P66 did not require the free 3′-end of DNA/RNA helix for its binding, we represented the data using 3′-biotinylated oligonucleotides.

To prove that topoisomerase I did not directly bind to SL1 RNA, P66 was continuously applied to the system following topoisomerase I (Fig. 3A). The plateau curve of the sensorgram during the topoisomerase I treatment indicated that topoisomerase I did not bind to SL1 RNA in the sensor chip. In contrast, P66 after topoisomerase I treatment bound to the sensor chip in a manner similar to that shown in Figs. 2B–D, indicating that topoisomerase I did not affect the binding of P66 to SL1 RNA. Next, we examined whether P66 could bind to SL1 RNA in the presence of topoisomerase I. As shown in Fig. 3B, P66 could combine with SL1 RNA even in the presence of topoisomerase I (Fig. 3B). Taken together, topoisomerase I did not inhibit the binding of P66; however, the bound P66 was dissociated from SL1 RNA by topoisomerase I.

We determined the dissociation rate by continuous injection of topoisomerase I. The dissociation rate constant (k_d) of P66 by topoisomerase I was calculated from curves of sensorgrams with different concentrations of topoisomerase I using the following kinetics evaluation software: a (500 pg/μl of topoisomerase I), $k_d = 9.45 \pm 0.36 \times 10^{-3}\,s^{-1}$; b (50 pg/μl of topoisomerase I), $3.55 \pm 0.04 \times 10^{-3}\,s^{-1}$; and c (buffer only), $3.08 \pm 0.03 \times 10^{-3}\,s^{-1}$ (Fig. 3C). We found that the k_d value of P66 in the presence of 500 pg/μl topoisomerase I was about 3 times higher than that in the absence of topoisomerase I, suggesting that P66 strongly bound to SL1 RNA.

Zinc finger domains of HIV-1 gag proteins are known to bind with genomic RNAs to carry them into virions. We next analyzed whether topoisomerase I dissociated gag proteins from the gag protein–RNA complex using the same system. Although Gag proteins bound to SL1 RNA, topoisomerase I did not affect the gag protein–RNA complex at all (Fig. 4A). We next

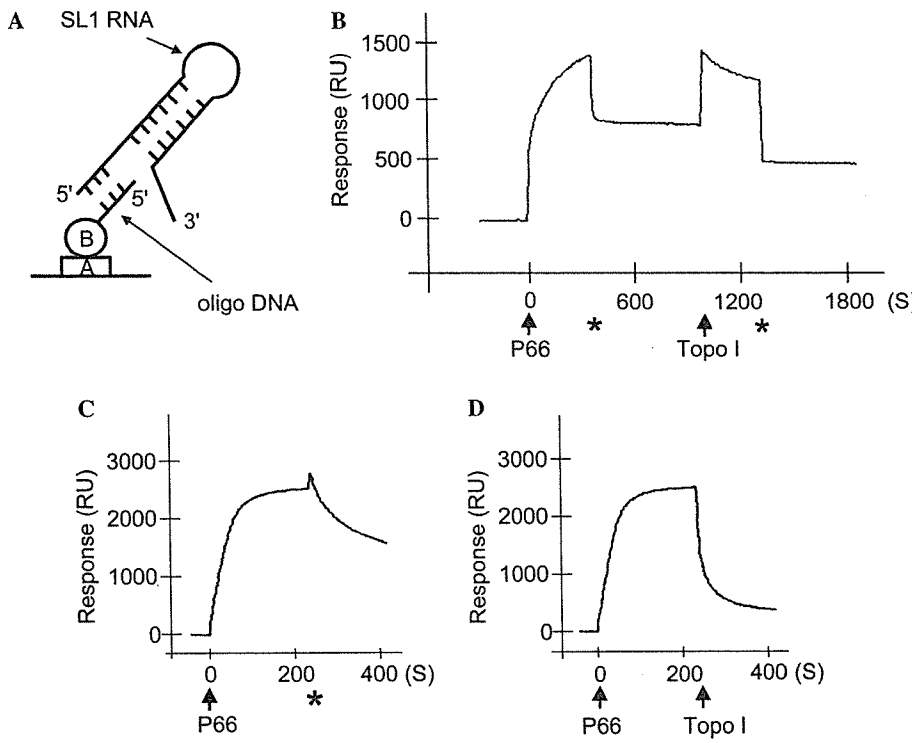

Fig. 2. Analysis of interaction among P66, SL1 RNA, and topoisomerase I using the surface plasmon resonance change. (A) A schematic figure of SL1 RNA substrate immobilized on the surface chip of the BIAcore system. Characters A and B represent avidin and biotin, respectively. Oligonucleotide was biotinylated at the 3′-end and prehybridized with SL1 RNA. (B) A representative sensorgram of three experiments illustrating the real-time binding of P66 (200 pg/μl) and dissociation of P66 by injection of topoisomerase I (500 pg/μl). Arrows indicate the initiation of injection of the purified P66 and topoisomerase I (Topo I). Asterisks indicate the end of the injection. The vertical and horizontal axes represent relative amounts of RT bound to immobilized RNA [Response, plasmon resonance units (RU)] and time [seconds (s)], respectively. (C,D) A representative sensorgram of three experiments illustrating the real-time binding and dissociation of P66 (200 pg/μl) (C) or further continuous injection of topoisomerase I (500 pg/μl) (D).

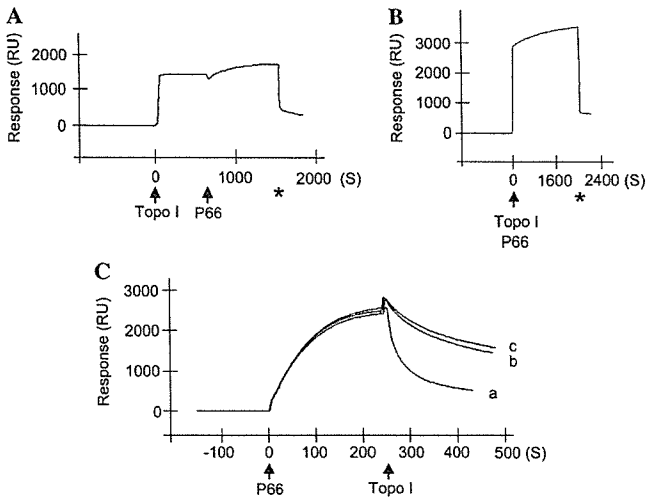

Fig. 3. Analysis of binding affinity of P66 to SL1 RNA in the presence of topoisomerase I using the surface plasmon resonance. (A) A representative sensorgram of two experiments illustrating the injection of P66 (200 pg/μl) after the injection of topoisomerase I (500 pg/μl). Arrows indicate the initiation of injection of the purified topoisomerase I (Topo I) and P66. Asterisks indicate the end of the injection. (B) A representative sensorgram of two experiments illustrating the coinjection of P66 (200 pg/μl) and topoisomerase I (500 pg/μl). (C) Representative overlay sensorgrams of three experiments illustrating the real-time binding and dissociation of P66 (200 pg/μl) in the presence of various concentrations of topoisomerase I (a, 500 pg/μl; b, 50 pg/μl; and c, 0 pg/μl).

applied murine leukemia virus (MuLV) RT and investigated the interaction between MuLV RT and human topoisomerase I. Although MuLV RT bound with SL1 RNA, topoisomerase I did not affect the binding of MuLV RT to SL1 RNA (Fig. 4B). Thus, it was suggested that topoisomerase I specifically dissociated the human P66 subunit of RT from the complex with SL1 RNA.

Discussion

In this study we demonstrated that topoisomerase I specifically dissociated P66, a subunit of HIV-1 RT, which strongly binds to structured RNAs. It has been reported that HIV-1 cDNA synthesis by RT pauses at the well-defined regions forming secondary structures, and efficient cDNA synthesis is limited to relatively short stretches of nucleotides lying in these sites [13]. Thus, cDNA synthesis during HIV-1 replication is considered to be much different from reverse transcription of heat-denatured RNA template. First, HIV-1 RNAs are fragmented in virions [11] and we found RNA ligase activity of cellular topoisomerase I played a pivotal role in cDNA synthesis [5]. Second, in addition to polymerase-dependent P66 at the 3′-end of primer, polymerase-independent P66 recognizing 5′-end or helix formation of structured RNA affects the reverse transcription of HIV-1 RNA. In RNA/DNA hybrids helix structure was reported to promote the binding of RT and RT measures the distance from the point of hybridization even in the case 3′-end of primer was unannealed [14,15]. Such tight binding of RT to the structured RNAs would inhibit polymerization of RNA. Therefore not only the RNA ligase activity of topoisomerase I but also the dissociation of polymerase-independent RT by topoisomerase I plays an important role in cDNA synthesis. Topoisomerase I is necessary for the adjustment of condition of RNA template during polymerization.

The specificity of dissociation of HIV-1 RT from SL1 RNA by topoisomerase I might partly explain the narrow host range of the HIV-1 tropism. Because topoisomerase I of African green monkey clearly suppressed cDNA synthesis of HIV-1 [9], the activity of human topoisomerase I including the dissociation of P66 from RNA template and

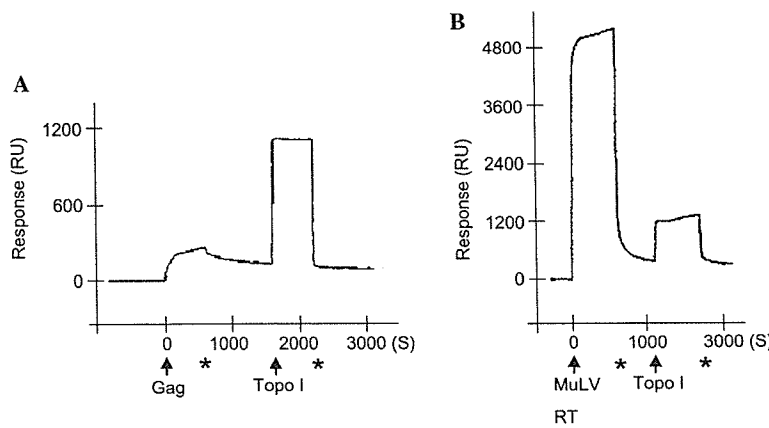

Fig. 4. Analysis of interaction of various RNA-binding proteins and topoisomerase I using the surface plasmon resonance. (A,B) Sensorgrams illustrating the real-time binding of GST-gag proteins (Gag) (50 pg/μl) (A) or MuLV RT (200 pg/μl) (B) in the presence of topoisomerase I (Topo I) (500 pg/μl). Arrows indicate the initiation of injection of Gag (A) or MuLV RT (B) and Topo I (A,B). Asterisks indicate the end of the injection. The vertical and horizontal axes represent relative amounts of Gag, MuLV RT or topoisomerase I bound to the immobilized RNA [Response, plasmon resonance units (RU)] and time (seconds (s)), respectively.

religation of nicked RNA genome would determine the effectivity of cDNA synthesis.

Thus, the binding of polymerase-independent RT to genomic RNA seems to be important for the inhibition of HIV-1 replication. It is expected that drugs which interfere with the association of RT and cellular topoisomerase I and do not inhibit topoisomerase I itself could be useful for the treatment of HIV-1 infection. Moreover, such drugs could be associated with the low frequency of the appearance of escape mutants. Future studies should determine the potential therapeutic role of such agents.

Acknowledgments

This work was supported in part by grants from the Ministry of Education, Science, Technology, Sports and Culture, and by grants from the Ministry of Health, Labor and Welfare, Japan, and the Japanese Foundation for AIDS Prevention.

References

[1] J. Hansen, T. Schulze, W. Mellert, K. Moelling, Identification and characterization of HIV-specific RNase H by monoclonal antibody, EMBO J. 7 (1988) 239–243.

[2] H. Ben Artzi, E. Zeelon, S.F. Le Grice, M. Gorecki, A. Panet, Characterization of the double stranded RNA dependent RNase activity associated with recombinant reverse transcriptases, Nucleic Acids Res. 20 (1992) 5115–5118.

[3] Z. Hostomsky, S.H. Hughes, S.P. Goff, S.F. Le Grice, Redesignation of the RNase D activity associated with retroviral reverse transcriptase as RNase H, J. Virol. 68 (1994) 1970–1971.

[4] E. Priel, S.D. Showalter, M. Roberts, S. Oroszlan, S. Segal, M. Aboud, D.G. Blair, Topoisomerase I activity associated with human immunodeficiency virus (HIV) particles and equine infectious anemia virus core, EMBO J. 9 (1990) 4167–4172.

[5] H. Takahashi, H. Sawa, H. Hasegawa, Y. Shoya, T. Sata, W.W. Hall, K. Nagashima, T. Kurata, Topoisomerase I and ATP activate cDNA synthesis of human immunodeficiency virus type 1, Biochem. Biophys. Res. Commun. 294 (2002) 509–517.

[6] H. Takahashi, H. Sawa, H. Hasegawa, T. Sata, W. Hall, T. Kurata, Binding and dissociation of human topoisomerase I with hairpin-loop RNAs: implications for the regulation of HIV-1 replication, Biochem. Biophys. Res. Commun. 297 (2002) 593–599.

[7] J.H. Weis, A.J. Faras, DNA topoisomerase activity associated with Rous sarcoma virus, Virology 114 (1981) 563–566.

[8] H. Takahashi, M. Matsuda, A. Kojima, T. Sata, T. Andoh, T. Kurata, K. Nagashima, W.W. Hall, Human immunodeficiency virus type 1 reverse transcriptase: enhancement of activity by interaction with cellular topoisomerase I, Proc. Natl. Acad. Sci. USA 92 (1995) 5694–5698.

[9] Y. Shoya, K. Tokunaga, H. Sawa, M. Maeda, T. Ueno, T. Yoshikawa, H. Hasegawa, T. Sata, T. Kurata, W.W. Hall, B.R. Cullen, H. Takahashi, Human topoisomerase I promotes HIV-1 proviral DNA synthesis: implications for the species specificity and cellular tropism of HIV-1 infection, Proc. Natl. Acad. Sci. USA 100 (2003) 8442–8447.

[10] A. Adachi, H.E. Gendelman, S. Koenig, T. Folks, R. Willey, A. Rabson, M.A. Martin, Production of acquired immunodeficiency syndrome-associated retrovirus in human and nonhuman cells transfected with an infectious molecular clone, J. Virol. 59 (1986) 284–291.

[11] H. Takahashi, H. Sawa, H. Hasegawa, T. Sata, W.W. Hall, K. Nagashima, T. Kurata, Reconstitution of cleavage of human immunodeficiency virus type-1 (HIV-1) RNAs, Biochem. Biophys. Res. Commun. 293 (2002) 1084–1091.

[12] L.G. Fagerstam, A. Frostell-Karlsson, R. Karlsson, B. Persson, I. Ronnberg, Biospecific interaction analysis using surface plasmon resonance detection applied to kinetic, binding site and concentration analysis, J. Chromatogr. 597 (1992) 397–410.

[13] G.J. Klarmann, C.A. Schauber, B.D. Preston, Template-directed pausing of DNA synthesis by HIV-1 reverse transcriptase during polymerization of HIV-1 sequences in vitro, J. Biol. Chem. 268 (1993) 9793–9802.

[14] C. Palaniappan, J.K. Kim, M. Wisniewski, P.J. Fay, R.A. Bambara, Control of initiation of viral plus strand DNA synthesis by HIV reverse transcriptase, J. Biol. Chem. 273 (1998) 3808–3816.

[15] C. Palaniappan, G.M. Fuentes, L. Rodriguez-Rodriguez, P.J. Fay, R.A. Bambara, Helix structure and ends of RNA/DNA hybrids direct the cleavage specificity of HIV-1 reverse transcriptase RNase H, J. Biol. Chem. 271 (1996) 2063–2070.

Microbiol. Immunol., **48**(2), 111–118, 2004

Nucleolin and the Packaging Signal, ψ, Promote the Budding of Human Immunodeficiency Virus Type-1 (HIV-1)

Tomonori Ueno[1,2], Kenzo Tokunaga[1], Hirofumi Sawa[3], Masae Maeda[1,3], Joe Chiba[2], Asato Kojima[1], Hideki Hasegawa[1], Yuko Shoya[1], Tetsutaro Sata[1], Takeshi Kurata[1], and Hidehiro Takahashi*[,1]

[1]*Department of Pathology, National Institute of Infectious Diseases, Shinjuku-ku, Tokyo 162–8640, Japan,* [2]*Department of Biological Science and Technology, Science University of Tokyo, Noda, Chiba 278–8510, Japan, and* [3]*Laboratory of Molecular and Cellular Pathology, 21st Century COE Program for Zoonosis Control, Hokkaido University School of Medicine, Sapporo, Hokkaido 060–8638, and CREST, JST, Japan*

Received September 17, 2003. Accepted November 17, 2003

Abstract: **Gag proteins of human immunodeficiency virus type 1 (HIV-1) play a pivotal role in the budding of the virion, in which the zinc finger motifs of the gag proteins recognize the packaging signal of genomic RNA. Nucleolin, an RNA-binding protein, is identified as a cellular protein that binds to murine leukemia virus (MuLV) gag proteins and regulates the viral budding, suggesting that HIV-1 gag proteins, the packaging signal, ψ and nucleolin affect the budding of HIV-1. Here we report that nucleolin enhances the release of HIV-1 virions which contain ψ. Furthermore, nucleolin and gag proteins form a complex incorporated into virions, and nucleolin promotes the infectivity of HIV-1. Our results suggest that an empty particle which contains neither nucleolin nor the genomic RNA is eliminated during the budding process, and this mechanism is beneficial for escape from the host immune response against HIV-1.**

Key words: **HIV-1, Nucleolin, Budding, Gag, Packaging signal**

The HIV-1 genome consists of three major genes: *gag*, *pol* and *env* (17). The *gag* gene is translated into a polyprotein that is sufficient to mediate the formation of virion-like particles (VLP) in the absence of other viral proteins (1). Gag precursor proteins ($Pr55^{gag}$) are subsequently cleaved into their structural component proteins including p17 matrix (MA), p24 capsid (CA), and p15 proteins. It has been reported that the p15 proteins are further cleaved into nucleocapsid (NC) p7 and p6 proteins. The NCp7 protein, which contains two zinc finger motifs thought to be important for packaging of the virus genomic RNA, binds to genomic RNA (10), mediates dimerization of the viral RNA, and promotes the annealing of a transfer RNA (tRNA) primer to the viral RNA genome. These zinc finger motifs are able to recognize the HIV-1 RNA packaging signal, forming a stem-loop structure which flanks the major subgenomic splice donor (12). Both the myristate and the basic motif signal at the N-terminal Gag sequence function as a targeting signal, which is essential for the proper assembly and budding of viral particles, to direct interaction with acidic phospholipids on the cytoplasmic leaflet of the plasma membrane (25).

As a host protein that binds to murine leukemia virus (MuLV) Gag, a nucleolin in which the carboxyl-terminal fragment interacts with the NC domain of MuLV Gag proteins has been identified by a yeast two-hybrid assay, and was shown to inhibit the assembly of viral virions (5). It has also been reported that a single point mutation adjacent to the capsid (CA)-nucleocapsid (NC) boundary of MuLV Gag diminished viral assembly, suggesting that the CA-NC junction is important for viral assembly.

Nucleolin, which contains four consensus RNA-binding domains, is one of the major non-ribosomal proteins in the nucleolus and is presumed to function in ribosomal DNA (rDNA) transcription, ribosomal RNA (rRNA) packaging, ribosome assembly and nucleo-cytoplasmic transport (18, 19). Structural and mutagenesis

**Address correspondence to* Dr. Hidehiro Takahashi, Department of Pathology, National Institute of Infectious Diseases, Toyama 1–23–1, Shinjuku-ku, Tokyo 162–8640, Japan. Fax: +81–3–5285–1189. E-mail: htakahas@nih.go.jp

Abbreviations: ELISA, enzyme-linked immunosorbent assay; HIV-1, human immunodeficiency virus type 1; RT, reverse transcriptase; rVV, recombinant vaccinia virus; VLP, virion-like particle.

studies have shown that nucleolin interacts specifically with a stem-loop RNA structure (3, 19). It has also been reported that nucleolin is expressed on the cellular surface as well as the intracellular pool within the nucleus and cytoplasm as a shuttle protein (21), and that cellular surface nucleolin and lipid rafts are implicated in early events in the HIV entry process (16).

In this study, we have examined whether nucleolin which are bound to HIV-1 gag proteins can regulate the budding of HIV-1. Nucleolin enhanced the release of both virion-like particles (VLPs) and HIV-1 virions in the presence of the RNA packaging signal, ψ, and form a complex with gag proteins incorporated into the virions. Furthermore, nucleolin promoted the infectivity of HIV-1, suggesting that an empty particle which contains neither nucleolin nor genomic RNA is eliminated during the budding process.

Materials and Methods

Cells and tissue culture. Human cervical carcinoma cells, HeLa cells (JCRB 9004), were provided from the Health Science Research Resources Bank (HSRRB, Japan). MAGIC5 cells which express human CD4 and human CCR5 and are derived from HeLa cells (14) were grown in Dulbecco's modified essential medium (DMEM) supplemented with 10% fetal bovine serum (FBS) at 37 C in an atmosphere of 5% CO_2. Rabbit kidney cells, RK13 cells (CCL-37), were purchased from the American Type Culture Collection (ATCC, ML). RK13 cells and human osteosarcoma lacking thymidine kinase cells, 143TK− cells, were grown in modified essential medium (MEM) supplemented with 10% fetal bovine serum at 37 C in an atmosphere of 5% CO_2.

Plasmid constructions. It has been reported that the nucleocapsid (NC) domains of Gag bind to a packaging signal which is a ~110 nucleotide segment of the genome known as the ψ-site. The HIV-1 ψ-site contains four stem-loops (SL1 through SL4), all of which are important for genome packaging (4). In order to eliminate the influence of viral proteins on the budding of virions after packaging, mutant HIV-1 was synthesized by *in vitro* mutagenesis. HIV-1 infectious DNA, pNL43 (2), was truncated between *Apa*I and *BamH*I sites for elimination of all the HIV-1 proteins including Pol, Vif, Vpr, Vpu, Tat, Rev, Env and Nef, and the first ATG codon of Gag was replaced with TTG, designated as ψ (+) DNA (Fig. 1). Alternatively, we made another HIV-1 mutant lacking a packaging signal, the ψ-site. To remove the packaging signal, a further truncation of the sequence 5′-TAC GCC AAA AAT TTT GAC TAG CGG GAG GCT AGA AGG AGA G-3′ (749–787 nt) was conducted by replacing the *BssH*II-*Sph*I fragment with a DNA fragment which was amplified from pNL43 with primers: 5′-GCT GAA GCG CGC ACG GCA AGA GGC GAG GGG CGG CGA CTG GTG AGA GTT GGG TGC GAG AGC GTC GGT ATT AAG CGG GGG AGA-3′ (705–824 nt) (underlining denotes *BssH*II and mutated ATG site) and 5′-ATG TCA CTT CCC CTT GGT TCT CTC-3′ (1473–1496 nt) and digested with *BssH*II and *Sph*I. The obtained vector was designated as ψ (−) DNA. Similarly, the *BssH*II-*Sph*I fragment of pNL43 was replaced with a *BssH*II-*Sph*I fragment containing the deleted packaging signal and the unmutated ATG codon, and was designated as ψ−. Mammalian expression vector encoding mouse Cyclin T1 mutated at 261-Tyrosine to Cystein, Y261C was obtained from Dr. Bieniasz (6).

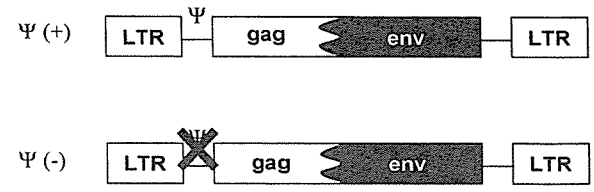

Fig. 1. Structure of plasmid producing HIV-1 truncated genomic RNA. ψ (+) and ψ (−) represent plasmids encoding HIV-1 LTR and provirus truncated between *gag* and *env*, with or without the packaging signal, respectively.

Human nucleolin cDNA (20) was amplified from HeLa cell cDNA (Clontech) by polymerase chain reaction (PCR) with primers NucF (5′-CAC TCC GCC GGA TCC ATG GTG AAG CTC GCG AA-3′) and NucR (5′-GCA GAG GGA TCT AGA CTA TTC AAA CTT CGT-3′) (underlining denotes *BamH*I and *Xba*I recognition sites). The PCR product digested by *BamH*I and *Xba*I was subcloned into a mammalian expression vector, pcDNA4/HisMaxC (Invitrogen) and designated as pchNuc.

Adenovirus and vaccinia virus vector. Recombinant adenovirus was synthesized following the manufacturer's instructions (Clontech). Briefly, the mammalian expressing vector pchNuc was digested by *Xba*I and *BamH*I and the digested fragment was subcloned into a shuttle vector, pTRE-Shuttle (Clontech), followed by digestion with I-*Ceu*I and *PI-Sce*I. The DNA fragment was ligated with linearized Adeno-X viral DNA (Clontech) and transformed into *E. coli*. The recombinant adenoviral DNA was extracted from *E. coli* and digested by *Pac*I followed by transfection to HEK293 cells by Fugene 6 (Roche). The adenovirus in the supernatant of the culture was amplified by recycling infection with HEK293 cells, and used infected to RK13 cells at 5 m.o.i. to express human nucleolin.

Recombinant vaccinia virus expressing $Pr55^{gag}$ (rVV-$Pr55^{gag}$) was constructed as described previously (22).

Briefly, a PCR fragment amplified from pNL43 with primers 55F (5'-AGA AGG AGA CCA TGG TGC GAG AGC GTC G-3') and 55R (5'-ATT GCC CCC GGA TCC TTA TTG TGA CGA GGG GTC-3') (underlining denotes *Nco*I and *BamH*I recognition sites) was digested with *Nco*I and *BamH*I, followed by a subcloning into pAK10 (9). Thymidine kinase-negative (TK−) viruses were isolated by plaque assay on 143TK− cells (9) in the presence of 5-bromo-2'-deoxyuridine at a concentration of 25 μg/ml, and were designated as pAKP55. The rVV-Pr55^{gag} was amplified by infection with RK cells, and used infected to RK13 cells at 5 m.o.i. to express Pr55^{gag} proteins.

Preparation of virion-like particles (VLPs) and HIV-1 virion. To prepare VLPs, RK13 cells were infected with the rVV-Pr55^{gag} with 5 m.o.i. at 37 C for 60 min. After washing with MEM-2% FBS, the cells were cultured in MEM-5% FBS. For HIV-1 virion stock, HeLa cells were transfected with HIV-1 provirus, pNL43 (2) using Fugene 6 (Roche). Either 24 hr after infection with rVV-Pr55^{gag} or 48 hr after transfection with pNL43, the culture supernatant was collected from each plate and centrifugated at 1,500×*g* for 10 min. After filtration to remove cell debris with a 0.45 μm filter, virion-like particles (VLPs) or viral virions were purified through a 25% sucrose cushion by centrifugation at 100,000×*g* for 2 hr and further isolated on 20 to 60% continuous sucrose gradients by centrifugation at 80,000×*g* at 4 C for 16 hr. The concentrations of VLPs or virions were estimated by measurement of p24 Gag antigen with an enzyme-linked immunosorbent assay (ELISA) (ZeptoMetrix, U.S.A.).

Each 0.5 ml of fraction was collected, and proteins in each fraction were precipitated with trichloroacetic acid in the presence of 1 mg of bovine serum albumin.

Immunoblotting. To estimate the efficiency of the HIV-1 budding from the cells, the amounts of Pr55^{gag} were examined by immunoblotting. For RK13 cells were infected with recombinant adenovirus encoding human nucleolin cDNA, and were thereafter transfected with the plasmids which transcribe a truncated HIV-1 genomic RNA with or without RNA packaging signal, designated as ψ (+) or ψ (−), respectively (Fig. 1). Forty-eight hr after transfection the cells were infected with the rVV-Pr55^{gag}. The amounts of gag proteins in the cells and supernatants were examined by immunoblotting 24 hr after infection. The virion-like particles (VLPs) in the supernatant was purified by ultracentrifugation at 50,000×*g* for 1 hr.

Collected samples were lysed with sodium dodecyl sulfate (SDS) sample buffer containing 2% (w/v) SDS, 63 mM Tris-HCl (pH 6.8), 10% (v/v) glycerol, 5% (v/v) 2-mercaptoethanol and 30 mM bromophenol blue, and sonicated. The samples were separated by SDS-PAGE and transferred to a polyvinylidene difluoride (PVDF) membrane, Immobilon (Millipore). For detection of exogenously expressed proteins, anti-p24 (1E4), anti-p17 (4D9) (9) or anti-nucleolin mouse monoclonal antibodies (Santa Cruz) were used as the primary antibodies, and horse-radish protein (HRP)-conjugated sheep anti-mouse IgG antibody as the second antibody. An ECL immunoblotting kit (Amersham Pharmacia Biotech) was used to visualize the detected proteins.

RT-PCR. From fractions separated from sucrose density gradient, RNAs were also extracted by an RNA extraction kit (Qiagen). After reverse transcriptase (RT) treatment, a real-time PCR was performed with primers NL-R 1F (5'-CTC TCT GGT TAG ACC AGA TCT GAG CCT GGG-3') (corresponding to 458–487 nt of pNL43, Gene Bank accession number, M19921) and NL-U51R (5'-ACT GCT AGA GAT TTT CCA CAC TGA CTA AAA-3') (607–636 nt). PCR was carried out in 20 μl total reaction volume with a LightCycler-RNA amplification kit (Roche), using a LightCycler (Roche). PCR conditions were as follows: 95 C for 5 min, followed by 50 cycles at 94 C for 15 sec, at 55 C for 20 sec, at 72 C for 15 sec, and a final extension at 72 C for 7 min. The relative amounts of genomic RNA were represented by the ratio of the amount against that of fraction 1, and were represented in a bar graph.

Immunoprecipitation of nucleolin-gag protein complex. RK13 cells (3×10^6) were transfected with 1 μg of pch-Nuc by using Fugene 6, 24 hr after infection with rVVpr55^{gag}. Twenty-four hr post transfection, cells were washed three times with cold PBS, swollen in 1 ml of hypotonic buffer (10 mM Tris-HCl, pH 7.4, 1 mM $MgCl_2$), and disrupted by a 15 ml Dounce tissue grinder with a tight pestle (Wheaton, NJ). Cell extracts were subjected to centrifugation at 1,000×*g* at 4 C for 10 min to sediment nuclei, followed by centrifugation at 10,000×*g* at 4 C for 10 min to precipitate organelles and cytoskeleton components. The soluble fraction obtained (S10) was analyzed by immunoprecipitation followed by SDS-PAGE and immunoblotting with the antibodies described in the text.

Luciferase reporter virus assay. In order to prepare virus stock, 2×10^5 of RK13 cells were transfected with 1 μg of an HIV-1 clone DNA based on the NL-43, pNL-Luc-E+R+, in which the *env* and *vpr* genes were intact and the *nef* gene was replaced with the firefly luciferase gene (7, 23) and with 0.5 μg of human nucleolin (pch-Nuc) and mutant cyclin T1-expressing plasmids by Fugene 6, following the manufacturer's instructions. The culture supernatants were harvested 48 hr after transfection and normalized as the p24 antigen amount. Three hundred μl of the supernatant containing the recombinant luciferase reporter HIV-1 virus virions were

inoculated with 3×10^4 MAGIC5 cells, and after 48 hr the cells were lysed with 200 μl of a lysis buffer supplied in a luciferase assay system (Promega). The luciferase activity was determined with a Lumat LB 96V luminometer (Perkin Elmer).

Results

Promotion of the Budding of Both HIV-1 VLPs and HIV-1 Virion by Human Nucleolin and the RNA Packaging Signal, ψ

Initially, the effect of human nucleolin and the RNA packaging signal on the efficiency of budding of HIV-1 VLPs was examined by measurement of the amounts of $Pr55^{gag}$ in the cellular lysates and the supernatants of the RK13 cells. The cells were infected with recombinant adenovirus encoding human nucleolin cDNA or mock adenovirus, and transfected with the plasmids expressing a truncated HIV-1 genomic RNA lacking the coding regions of all the HIV-1 proteins with [ψ (+)] or without [ψ (−)] the RNA packaging signal, ψ (Fig. 1), followed with infection of recombinant vaccinia virus expressing HIV-1 $Pr55^{gag}$ (rVV-$Pr55^{gag}$). Exogenous human nucleolin did not affect the $Pr55^{gag}$ levels in the cell lysates in the presence or absence of ψ (Fig. 2A). On the contrary, nucleolin enhanced the amounts of $Pr55^{gag}$ in the supernatant (Fig. 2B). In addition, the amount of $Pr55^{gag}$ in the supernatant was also increased in the presence of ψ.

Next, we analyzed the effects of human nucleolin and ψ on the budding of native HIV-1 virion. RK-13 cells were cotransfected with pchNuc encoding human nucleolin cDNA or an empty vector and an HIV-1 clone DNA, pNL43 (ψ+) or without ψ (ψ−). The level of $Pr55^{gag}$ proteins in the supernatants from the cells was analyzed in a similar manner as that shown in Fig. 2. Neither human nucleolin nor ψ affected the cellular level of $Pr55^{gag}$ (Fig. 3A). In contrast, human nucleolin and ψ synergistically enhanced the release of $p24^{gag}$ in the supernatants (Fig. 3B). We also examined the effect of ψ in the human cell line HeLa cells, which express human nucleolin (Fig. 4, A and B). The protein expression levels of nucleolin were not significantly changed after transfection of the plasmid encoding human nucleolin cDNA in HeLa cells (data not shown). Although ψ did not affect the level of $Pr55^{gag}$ in the cells (Fig. 4A), the release level of p24 was enhanced in the presence of ψ in the supernatants (Fig. 4B). These results suggest that nucleolin enhanced the budding efficiency of VLPs and HIV-1 virions in the presence of ψ.

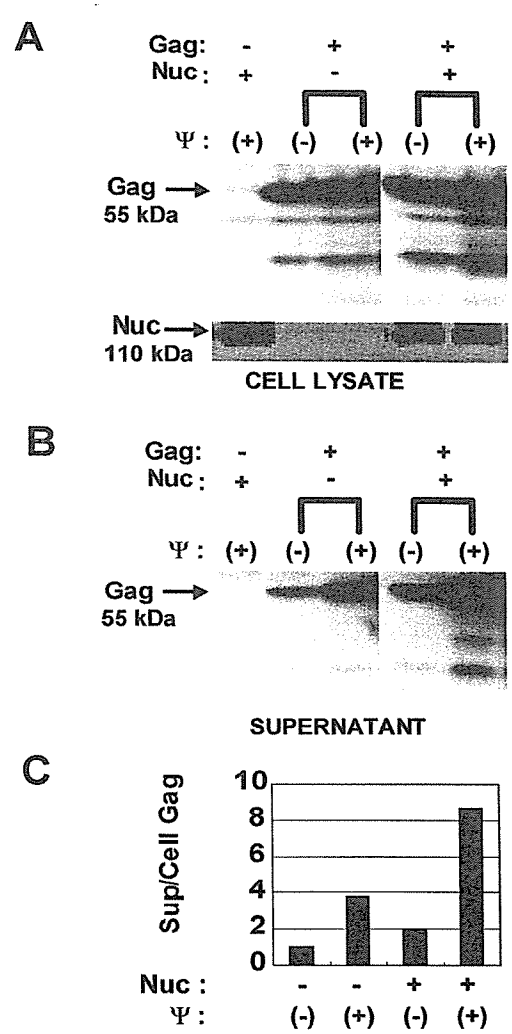

Fig. 2. Enhancement of the budding of VLPs by human nucleolin in the presence or absence of the RNA packaging signal, ψ, in RK13 cells. Cellular lysates (A) or supernatants (B) from RK13 cells expressing (Nuc+) or not expressing (Nuc−) human nucleolin which transiently expressed the truncated HIV-1 plasmid with [ψ (+)] or without [ψ (−)] RNA packaging signal, ψ, followed with (Gag+) or without (Gag−) infection of rVV-$Pr55^{gag}$, were analyzed by immunoblotting with both anti-gag and anti-nucleolin antibodies. Black arrows indicate the positions of $Pr55^{gag}$ (Gag) and nucleolin (Nuc). (C) The signal ratios of Gag proteins in supernatants to that in cell lysates were calculated and the fold increases (Sup/Cell Gag) to the lane without expression of both nucleolin and ψ are demonstrated as a column graph.

Enhancement of Incorporation of Nucleolin into the VLP with the Presence of ψ

Next, we analyzed whether nucleolin could be incorporated into VLPs. RK13 cells were transfected with pchNuc expressing human nucleolin, and a plasmid encoding ψ [ψ (+)] (Fig. 1) followed by infection with rVV-$Pr55^{gag}$. Because expression of Gag proteins by infection of rVV-$Pr55^{gag}$ produced a much higher amount in RK13 cells than transfection of pNL43, nucleolin or

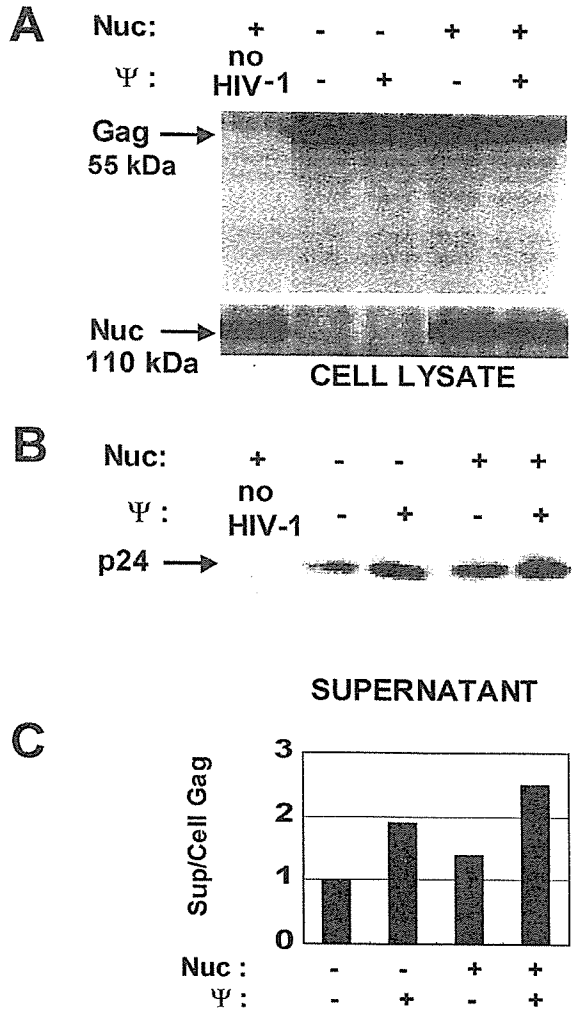

Fig. 3. Enhancement of the budding of HIV-1 virions by human nucleolin in the presence or absence of ψ in RK13 cells. Cellular lysates (A) or supernatants (B) from RK13 cells transfected with pchNuc expressing human nucleolin (Nuc+) or an empty vector (Nuc−) and an HIV-1 clone, pNL43 (ψ+) or pNL43 without ψ (ψ−) or without HIV clone (no HIV-1), were analyzed by immunoblotting with both anti-gag and anti-nucleolin antibodies. Black arrows indicate the positions of $Pr55^{gag}$ (Gag), nucleolin (Nuc) and p24. (C) The signal ratios of p24 proteins in supernatants to Gag proteins in cell lysates were calculated and the fold increases (Sup/Cell Gag) to the lane without expression of both nucleolin (Nuc−) and ψ (ψ−) are demonstrated as a column graph.

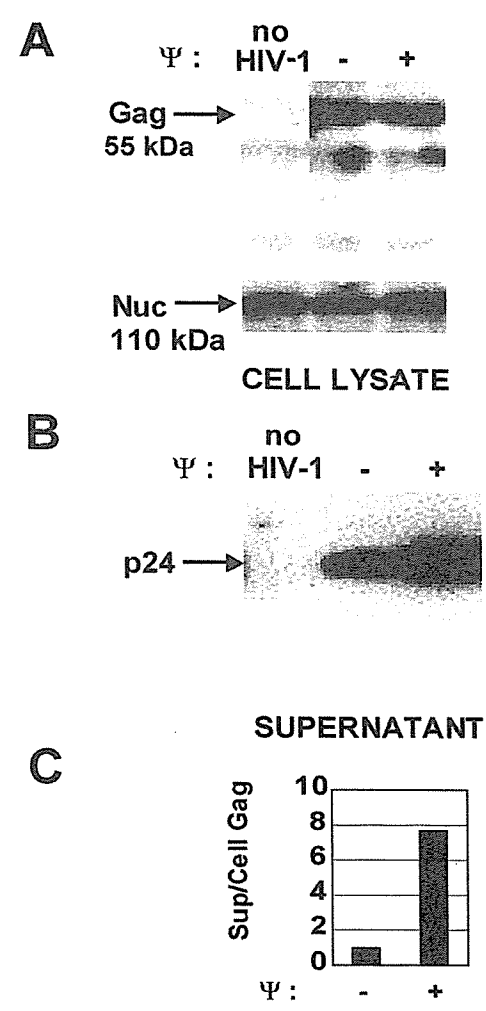

Fig. 4. Enhancement of the budding of HIV-1 virions in HeLa cells. Cellular lysates (A) or supernatants (B) from HeLa cells transfected with an HIV-1 clone, pNL43 (ψ+), pNL43 without ψ (ψ−) or not transfected (no HIV-1) were analyzed by immunoblotting with both anti-gag and anti-nucleolin antibodies. Black arrows indicate the positions of $Pr55^{gag}$ (Gag), nucleolin (Nuc) and p24. (C) The signal ratios of p24 proteins in supernatants to Gag proteins in cell lysates were calculated and the fold increases (Sup/Cell Gag) to the lane without expression of ψ (ψ−) are demonstrated as a column graph.

the packaging signal more effectively enhanced budding of virion when Gag proteins were expressed by rVV-$Pr55^{gag}$.

After fractionation of VLPs by sucrose density gradient, the amounts of gag proteins, nucleolin and genomic RNA in each fraction were examined. As shown in Fig. 5, a high expression level of human nucleolin was recognized in fractions 4, 5, and 6 (their sucrose concentrations being 35, 45, and 50, respectively), in which $Pr55^{gag}$ was also highly assembled. HIV-1 genomic RNA was highly assembled in fractions 5 and 6 (about a 5-fold increase in comparison to fraction 1) (Fig. 5).

To examine the role of ψ in the incorporation of human nucleolin into VLPs, RK13 cells were transfected with pchNuc expressing human nucleolin and a plasmid encoding [ψ (+)] or unencoding ψ [ψ (−)] (Fig. 1); thereafter, the cells were inoculated with rVV-$Pr55^{gag}$. Similarly as in Fig. 5, VLPs in the supernatants were separated by sucrose density gradient and 14 fractions were analyzed for gag proteins and human nucleolin. Gag proteins and human nucleolin were assembled in fractions 4,

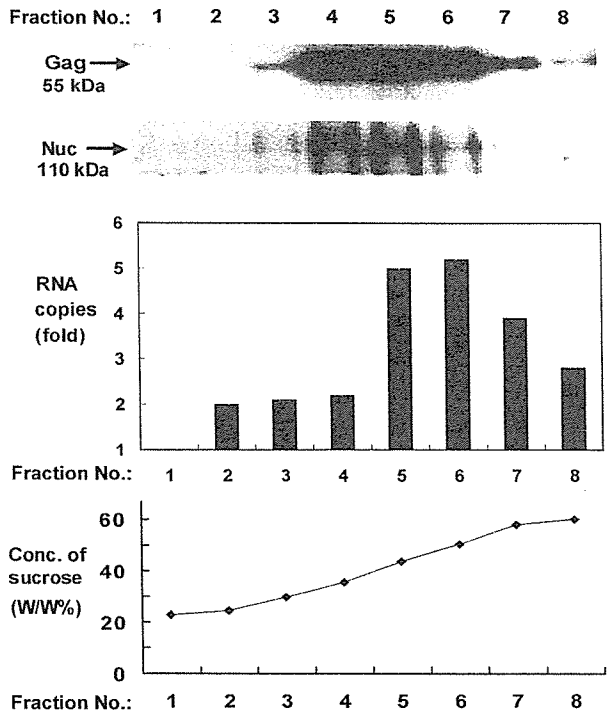

Fig. 5. Analysis of $Pr55^{gag}$, human nucleolin, and HIV-1 genomic RNA of fractionated supernatants from RK13 cells by sucrose density gradient. The supernatant from RK13 cells expressing human nucleolin and the truncated HIV-1 provirus with ψ (Fig. 1) followed by infection with rVV-$Pr55^{gag}$ was separated by sucrose density gradient, and each fraction was analyzed by a real-time RT-PCR and immunoblotting with anti-nucleolin and anti-$Pr55^{gag}$ antibodies. Black arrows indicate the positions of $Pr55^{gag}$ (Gag) and nucleolin (Nuc). The relative amounts of genomic RNA are represented as the ratio of each amount to that of fraction 1, and are shown in the form of the bar graph. The concentrations of sucrose [conc. of sucrose (w/w %)] are represented in the line graph.

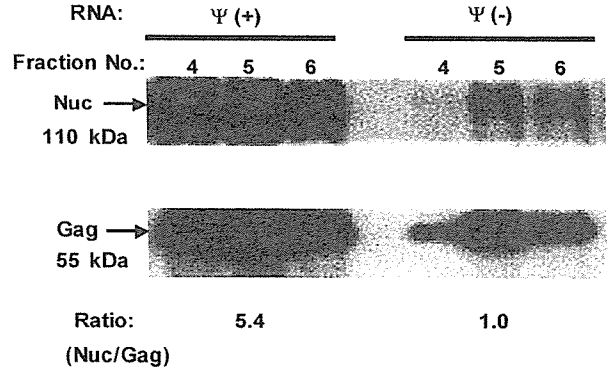

Fig. 6. Incorporation of nucleolin into VLPs with or without ψ. The supernatant from RK13 cells expressing human nucleolin and the truncated HIV-1 provirus with ψ [ψ (+)] (Fig. 1) or without ψ [ψ (−)] followed by infection with rVV-$Pr55^{gag}$ was separated by sucrose density gradient, and each fraction was analyzed by immunoblotting with anti-nucleolin and anti-gag antibodies. The results of fractions 4, 5, and 6 are shown. Black arrows indicate the positions of $Pr55^{gag}$ (Gag) and nucleolin (Nuc). The ratios of signal intensity of nucleolin to gag proteins (Nuc/Gag) in fraction 5 are indicated below the immunoblot.

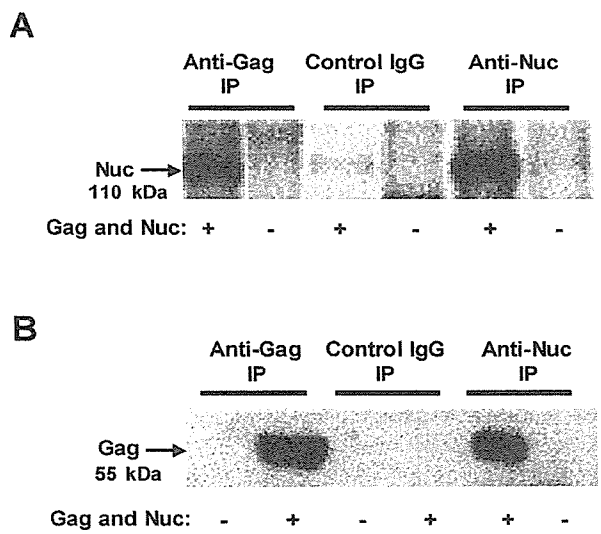

Fig. 7. Co-immunoprecipitaiton of gag proteins and nucleolin in RK13 cells. Cellular lysates from RK13 cells transfected with pch-Nuc expressing human nucleolin and infected with rVV$pr55^{gag}$ (Gag and Nuc+) or neither transfected nor infected (Gag and Nuc−), were immunoprecipitated (IP) with anti-gag (Anti-Gag), anti-nucleolin (Anti-Nuc) antibodies or control immunoglobulin G (IgG), and precipitated samples were immunoblotted with anti-nucleolin (A) and anti-gag (B) antibodies. Black arrows indicate the positions of $pr55^{gag}$ (Gag) and nucleolin (Nuc).

5, and 6 (Fig. 6). In the presence of ψ, the ratio of the signal intensity of nucleolin to Gag proteins was 5.4 times more than that in the absence of ψ (Fig. 6). These results demonstrate that human nucleolin was incorporated into VLPs with HIV-1 genomic RNA, and that the efficiency of the incorporation was enhanced in the presence of ψ.

The Binding of Human Nucleolin and Gag Proeins

To analyze whether human nucleolin can bind HIV-1 gag proteins in a manner similar to that previously reported about mouse nucleolin and MuLV gag proteins (5), a human nucleolin-expressing vector was transfected into RK13 cells, following by infection of rVV-$Pr55^{gag}$. Immunoprecipitaiton analysis of the cell lysates demonstrated that gag proteins and nucleolin were co-immunoprecipitated (Fig. 7, A and B), suggesting that human nucleolin binds to HIV-1 gag proteins *in vivo*.

Enhancement of HIV-1 Infectivity by Human Nucleolin

Finally, we examined whether nucleolin enhances the infectivity of HIV-1. A luciferase reporter HIV-1-producing vector, pNL-Luc-E+R+, in which the *nef* gene was replaced by the luciferase gene and a human nucle-

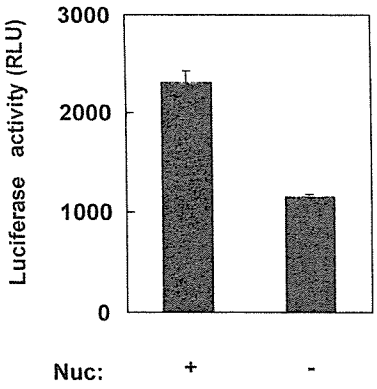

Fig. 8. The effect of nucleolin against HIV-1 infectivity. Supernatants from RK13 cells transfected with pNL-Luc-E+R+ in which the *nef* gene was replaced with the firefly luciferase gene, and pchNuc expressing human nucleolin (Nuc+) or an empty vector (Nuc−) were normalized as the p24 antigen amount and inoculated to MAGIC5 cells and luciferase activities were measured as a relative luciferase activity unit (RLU).

olin-expressing vector (Nuc+) or an empty vector (Nuc−) was introduced into RK13 cells and the supernatant was normalized as the p24 antigen amount. The total infectivity represented by the luciferase activity of HIV-1 derived from cells expressing human nucleolin increased to about twice that from cells without nucleolin expression (Fig. 8), suggesting that human nucleolin enhanced the HIV-1 infectivity.

Discussion

In order to examine the relationships of the gag proteins, nucleolin and ψ to the infectivity of HIV-1, we initially analyzed the budding of gag proteins expressed by a recombinant vaccinia virus or HIV-1 provirus, and found that nucleolin and ψ synergistically enhanced the release of gag proteins. In addition, nucleolin and HIV-1 genomic RNA were incorporated into VLPs, and ψ enhanced the incorporation of nucleolin into VLPs.

The regulation of budding is considered to consist of the assembly of gag proteins at the plasma membrane and the release of virions (15). Recently, the assembly of gag proteins has been reported to be regulated by a cellular factor known as Tsg101, which belongs to the family of ubiquitin-conjugating enzymes (E2) and functions in vacuolar protein sorting. Tsg101 binds with HIV-1 $Pr55^{gag}$ and plays an important role in the assembly and budding of HIV-1 (8, 24). It has also been reported that HP68, a cellular ATP-binding protein, forms a complex with gag proteins and plays a critical role in HIV-1 assembly (26). Nucleolin regulates the construction of ribosomes, functions as a transporter protein between the nucleus and cytoplasm along the actin, and enhances the assembly of rRNA and ribosomal subunit proteins by binding at RNA binding domains and protein-binding domains, respectively (18, 19, 21). Although it is still unknown whether nucleolin interacts with Tsg101 or HP68, we supposed that nucleolin binds to gag proteins and ψ of HIV-1, and might be involved in the transfer of gag proteins from the nucleus to the cellular membrane. This idea was supported by several reports which stated that deleted nucleolin suppressed the budding of MuLV, HIV-1 nucleocapsid proteins bound with actin (11), and that murine nucleolin was incorporated to virions and colocalized with MuLV gag proteins (5).

The formation of nucleolin-gag protein complexes (Fig. 7) and incorporation of nucleolin (Figs. 5 and 6) into VLPs suggested that a nucleolin-gag protein complex seemed to be required for the release of virions. It has been reported that both gag proteins and nucleolin bind to a stem-loop structure in ψ (3, 10, 13, 19). Taken together, nucleolin, gag proteins and ψ might be necessary for the budding of HIV-1, and they might be incorporated into virions together. This mechanism might function to avoid the release of virions without carrying genomic RNA and to reduce the spreading of virions that cannot replicate but do enhance antigen presentation to the immune system.

In conclusion, our results provide evidence that the budding of HIV-1 gag proteins is regulated by nucleolin and ψ.

References

1) Accola, M.A., Strack, B., and Gottlinger, H.G. 2000. Efficient particle production by minimal Gag constructs which retain the carboxy-terminal domain of human immunodeficiency virus type 1 capsid-p2 and a late assembly domain. J. Virol. **74**: 5395–5402.
2) Adachi, A., Gendelman, H.E., Koenig, S., Folks, T., Willey, R., Rabson, A., and Martin, M.A. 1986. Production of acquired immunodeficiency syndrome-associated retrovirus in human and nonhuman cells transfected with an infectious molecular clone. J. Virol. **59**: 284–291.
3) Allain, F.H., Gilbert, D.E., Bouvet, P., and Feigon, J. 2000. Solution structure of the two N-terminal RNA-binding domains of nucleolin and NMR study of the interaction with its RNA target. J. Mol. Biol. **303**: 227–241.
4) Amarasinghe, G.K., Zhou, J., Miskimon, M., Chancellor, K.J., McDonald, J.A., Matthews, A.G., Miller, R.R., Rouse, M.D., and Summers, M.F. 2001. Stem-loop SL4 of the HIV-1 psi RNA packaging signal exhibits weak affinity for the nucleocapsid protein. Structural studies and implications for genome recognition. J. Mol. Biol. **314**: 961–970.
5) Bacharach, E., Gonsky, J., Alin, K., Orlova, M., and Goff, S.P. 2000. The carboxy-terminal fragment of nucleolin interacts with the nucleocapsid domain of retroviral gag proteins and inhibits virion assembly. J. Virol. **74**: 11027–11039.

6) Bieniasz, P.D., Grdina, T.A., Bogerd, H.P., and Cullen, B.R. 1998. Recruitment of a protein complex containing Tat and cyclin T1 to TAR governs the species specificity of HIV-1 Tat. EMBO J. **17**: 7056–7065.
7) Connor, R.I., Chen, B.K., Choe, S., and Landau, N.R. 1995. Vpr is required for efficient replication of human immunodeficiency virus type-1 in mononuclear phagocytes. Virology **206**: 935–944.
8) Garrus, J.E., von Schwedler, U.K., Pornillos, O.W., Morham, S.G., Zavitz, K.H., Wang, H.E., Wettstein, D.A., Stray, K.M., Cote, M., Rich, R.L., Myszka, D.G., and Sundquist, W.I. 2001. Tsg101 and the vacuolar protein sorting pathway are essential for hiv-1 budding. Cell **107**: 55–65.
9) Hoshikawa, N., Kojima, A., Yasuda, A., Takayashiki, E., Masuko, S., Chiba, J., Sata, T., and Kurata, T. 1991. Role of the gag and pol genes of human immunodeficiency virus in the morphogenesis and maturation of retrovirus-like particles expressed by recombinant vaccinia virus: an ultrastructural study. J. Gen. Virol. **72**: 2509–2517.
10) Khan, R. and Giedroc, D.P. 1992. Recombinant human immunodeficiency virus type 1 nucleocapsid (NCp7) protein unwinds tRNA. J. Biol. Chem. **267**: 6689–6695.
11) Liu, B., Dai, R., Tian, C.J., Dawson, L., Gorelick, R., and Yu, X.F. 1999. Interaction of the human immunodeficiency virus type 1 nucleocapsid with actin. J. Virol. **73**: 2901–2908.
12) McBride, M.S. and Panganiban, A.T. 1996. The human immunodeficiency virus type 1 encapsidation site is a multipartite RNA element composed of functional hairpin structures. J. Virol. **70**: 2963–2973.
13) Meric, C. and Goff, S.P. 1989. Characterization of Moloney murine leukemia virus mutants with single-amino-acid substitutions in the Cys-His box of the nucleocapsid protein. J. Virol. **63**: 1558–1568.
14) Mochizuki, N., Otsuka, N., Matsuo, K., Shiino, T., Kojima, A., Kurata, T., Sakai, K., Yamamoto, N., Isomura, S., Dhole, T.N., Takebe, Y., Matsuda, M., and Tatsumi, M. 1999. An infectious DNA clone of HIV type 1 subtype C. AIDS Res. Hum. Retroviruses **15**: 1321–1324.
15) Nisole, S., Krust, B., Callebaut, C., Guichard, G., Muller, S., Briand, J.P., and Hovanessian, A.G. 1999. The anti-HIV pseudopeptide HB-19 forms a complex with the cell-surface-expressed nucleolin independent of heparan sulfate proteoglycans. J. Biol. Chem. **274**: 27875–27884.
16) Nisole, S., Krust, B., and Hovanessian, A.G. 2002 Anchorage of HIV on permissive cells leads to coaggregation of viral particles with surface nucleolin at membrane raft microdomains. Exp. Cell Res. **276**: 155–173.
17) Ratner, L., Haseltine, W., Patarca, R., Livak, K.J., Starcich, B., Josephs, S.F., Doran, E.R., Rafalski, J.A., Whitehorn, E.A., and Baumeister, K. 1985. Complete nucleotide sequence of the AIDS virus, HTLV-III. Nature **313**: 277–284.
18) Roger, B., Moisand, A., Amalric, F., and Bouvet, P. 2002. Repression of RNA polymerase I transcription by nucleolin is independent of the RNA sequence that is transcribed. J. Biol. Chem. **277**: 10209–10219.
19) Serin, G., Joseph, G., Ghisolfi, L., Bauzan, M., Erard, M., Amalric, F., and Bouvet, P. 1997. Two RNA-binding domains determine the RNA-binding specificity of nucleolin. J. Biol. Chem. **272**: 13109–13116.
20) Srivastava, M., Fleming, P.J., Pollard, H.B., and Burns, A.L. 1989. Cloning and sequencing of the human nucleolin cDNA. FEBS Lett. **250**: 99–105.
21) Srivastava, M., and Pollard, H.B. 1999. Molecular dissection of nucleolin's role in growth and cell proliferation: new insights. FASEB J. **13**: 1911–1922.
22) Takahashi, H., Matsuda, M., Kojima, A., Sata, T., Andoh, T., Kurata, T., Nagashima, K., and Hall, W.W. 1995. Human immunodeficiency virus type 1 reverse transcriptase: enhancement of activity by interaction with cellular topoisomerase I. Proc. Natl. Acad. Sci. U.S.A. **92**: 5694–5698.
23) Tokunaga, K., Greenberg, M.L., Morse, M.A., Cumming, R.I., Lyerly, H.K., and Cullen, B.R. 2002. Molecular basis for cell tropism of CXCR4-dependent human immunodeficiency virus type 1 isolates. J. Virol. **75**: 6776–6785.
24) VerPlank, L., Bouamr, F., LaGrassa, T.J., Agresta, B., Kikonyogo, A., Leis, J., and Carter, C.A. 2001. Tsg101, a homologue of ubiquitin-conjugating (E2) enzymes, binds the L domain in HIV type 1 Pr55(Gag). Proc. Natl. Acad. Sci. U.S.A. **98**: 7724–7729.
25) Zhou, W., Parent, L.J., Wills, J.W., and Resh, M.D. 1994. Identification of a membrane-binding domain within the amino-terminal region of human immunodeficiency virus type 1 Gag protein which interacts with acidic phospholipids. J. Virol. **68**: 2556–2569.
26) Zimmerman, C., Klein, K.C., Kiser, P.K., Singh, A.R., Firestein, B.L., Riba, S.C., and Lingappa, J.R. 2002. Identification of a host protein essential for assembly of immature HIV-1 capsids. Nature **415**: 88–92.

Available online at www.sciencedirect.com
ScienceDirect
Microbes and Infection 8 (2006) 2647–2656
Microbes and Infection
www.elsevier.com/locate/micinf

Original article

Tristetraprolin inhibits HIV-1 production by binding to genomic RNA

Masae Maeda [a,b,c], Hirofumi Sawa [c,d,e], Minoru Tobiume [a], Kenzo Tokunaga [a], Hideki Hasegawa [a], Takeshi Ichinohe [a], Tetsutaro Sata [a], Masami Moriyama [b], William W. Hall [f], Takeshi Kurata [a], Hidehiro Takahashi [a,*]

[a] *Department of Pathology, National Institute of Infectious Diseases, Toyama 1-23-1, Shinjuku-ku, Tokyo 162-8640, Japan*
[b] *Department of Microbiology and Immunology, School of Medicine, Keio University, Tokyo, Japan*
[c] *CREST, JST, Japan*
[d] *Department of Molecular Pathobiology, Hokkaido University Research Center for Zoonosis Control, Hokkaido University, Sapporo, Japan*
[e] *21st Century COE Program for Zoonosis, Hokkaido University, Sapporo, Japan*
[f] *Department of Medical Microbiology, Conway Institute of Biomolecular and Biomedical Research, University College Dublin, Belfield, Dublin, Ireland*

Received 2 February 2006; accepted 18 July 2006
Available online 8 August 2006

Abstract

HIV-1 genome has an AU-rich sequence and requires rapid nuclear export by Rev activity to prevent multiple splicing. HIV-1 infection occurs in activated $CD4^+$ T cells where the decay of mRNAs of cytokines and chemokines is regulated by the binding of AU-rich elements to the mRNA-destabilizing protein tristetraprolin. We here investigated the influence of tristetraprolin on the replication of HIV-1. Treatment of siRNA against tristetraprolin in a latently HIV-1 infected cell line increases HIV-1 production following stimulation. A chloramphenicol acetyltransferase and luciferase assay revealed that exogenous tristetraprolin reduced HIV-1 virion production and in contrast increased the multiply spliced products. Furthermore, quantitative RT–PCR analysis showed tristetraprolin increases the ratio of multiple-spliced RNAs to un-, single-spliced RNA. Moreover, an electrophoretic mobility shift assay showed that tristetraprolin binds to synthesized HIV-1 RNA with AU-rich sequence but not to RNA with less AU sequence. These results suggest that tristetraprolin is a regulator of HIV-1 replication and enhances splicing by direct binding to AU-rich sequence of HIV-1 RNAs.

Keywords: Human immunodeficiency virus type 1; Tristetraprolin; AU-rich element

1. Introduction

Expression of human immunodeficiency virus type 1 (HIV-1) genes is regulated by several posttranscriptional mechanisms, which include RNA splicing, stability, transport and translation. For example, HIV-1 RNA contains inhibitory sequences (INS) negatively regulating expression [1], which is also known to be AU-rich [2]. Replacement of AU residues of HIV-1 mRNA has been reported to result in a marked increase in expression of HIV-1 Gag, Pol, and Env proteins independent of the Crm1/Rev/Rev-responsive element (RRE) export pathway [3]. In addition, another nuclear export system, constitutive transport elements (CTE)/Tap, can substitute Rev/RRE [4], suggesting that effective nuclear export is required to complement the character of AU-rich RNA genome. As we have previously reported that HIV-1 RNA is fragmented

Abbreviations: HIV-1, human immunodeficiency virus type 1; TTP, tristetraprolin; ARE, AU-rich element; RRE, Rev-responsive element; nt, nucleotide; RT, reverse transcription; PCR, polymerase chain reaction; CAT, chloramphenicol acetyltransferase; VSV-G, vesicular stomatitis virus envelope glycoprotein.

* Corresponding author. Tel.: +81 3 5285 1111; fax: +81 3 5285 1189.
E-mail address: htakahas@nih.go.jp (H. Takahashi).

1286-4579/$ - see front matter © 2006 Elsevier Masson SAS. All rights reserved.
doi:10.1016/j.micinf.2006.07.010

in viral particles and in vitro-synthesized HIV-1 RNA is cleaved between U and A or C and A [5], effective nuclear export of HIV-1 RNA by Crm1/Rev/RRE might be required to rescue a potentially unstable RNA genome, and the balance between RNA decay and nuclear export could be an important facet of HIV-1 replication and pathogenesis.

Whereas activated $CD4^+$ T cells are a primary target for productive HIV-1 infection [6], HIV-1 production does not occur in resting $CD4^+$ T cells because of a low level of reverse transcriptase activity [7]. In activated cells, including $CD4^+$ T cells that produce cytokines, chemokines and other proteins in response to inflammation and infection, mRNAs are degraded rapidly following transient activation [8]. These mRNAs contain the AU-rich element (ARE) in their 3′-untranslated region (3′UTR) that binds with tristetraprolin (TTP, also known as TIS11, Nup475, or G0S24) [9]. TTP is the prototype of a family of proteins that possess a pair of closely spaced zinc fingers of the CCCH class and are capable to binding AU-rich elements (ARE) in the 3′UTR and subsequent destruction of transcripts of pro-inflammatory mediators such as tumor necrosis factor α, granulocyte/macrophage colony stimulating factor, and cyclooxygenase 2 [10].

We propose the hypothesis that TTP might interact with the AU-rich regions of HIV-1 RNA and that the regulation of the HIV-1 RNA genome could play important roles in the post-transcriptional control of HIV-1 replication in activated or memory T cells. We show that TTP reduced HIV-1 virion production by enhancing multiple splicing through binding to HIV-1 AU-rich RNA.

2. Materials and methods

2.1. Cell culture

The human cell lines HEK293T and HeLa were maintained under an atmosphere of 5% CO_2 at 37 °C in Dulbecco's modified Eagle's medium supplemented with 10% fetal bovine serum. U1 cells [11] were cultured in complete medium (RPMI 1640 medium supplemented with 10% fetal bovine serum).

2.2. RNAi inhibition

siRNA treatment was achieved using synthetic oligonucleotides which were purchased from Ambion. Sense sequence of TTP siRNA is CCC AUA AAU CAA UGG GCC Ctt (small capital displays deoxyribonucleic acid) and antisense is GGG CCC AUU GAU UUA UGG Gtg. Two rounds of siRNA treatments were performed. siRNA was transfected by using the electric transfection apparatus, amaxa in U1 cells.

2.3. Cloning, mutagenesis, and plasmid construction for TTP or rev expression vectors

Polyadenylated RNA was isolated from HeLa cells and subjected to reverse transcription (RT) with SuperScript $RNaseH^-$ reverse transcriptase (Invitrogen Life Technologies) and a 15-nucleotide poly(dT) primer. The coding region of human TTP cDNA was amplified by polymerase chain reaction (PCR) with the reverse-transcribed cDNA as the template and with the primers 5′-CGT GAATTC ATG GAT CTG ACT GCC ATC TAC GAG AGC CT-3′ (TTPF, *Eco*RI site underlined) and 5′-GAC CGG GCA G GCGGCCGC TCA CTC AGA AAC AGA GAT-3′ (TTPR, *Not*I site underlined). The PCR product was digested with *Eco*RI and *Not*I and then cloned into pcDNA4/HisMax-C (Invitrogen Life Technologies), a mammalian expression vector containing the Xpress epitope tag sequence, or into pCAGGS-IRES-EGFP [12], yielding pchTTPwt or pCAGGSTTP, respectively. The resulting plasmids were sequenced with a DNA sequencer (model 377A; Perkin Elmer, Norwalk, CT). Expression vectors for TTP deletion mutants, including 1–101, 76–189, and 176–320, were similarly constructed with pchTTPwt as the template and with the primers 5′-TCT CTG AG GCGGCCGC TTA TAG CTC AGT CTT GTA GCG CGA -3′ (R1–101), 5′-CTG GCT GAATTC CTG GGC CCT GAG CTG TCA CCCT-3′ (F76–189), 5′-AGG CCT GGT GCGGCCGC TTA GGT CCG GCG GCC AGA GGG CA-3′ (R76–189), and 5′-CCT GTG GAATTC CAG AGC ATC AGC TTC TCC GGC CT-3′ (F176–320). The resulting expression vectors were designated pcD1–101, pcD76–189, and pcD176–320, respectively.

For construction of vectors for Xpress-tagged Rev, the Rev cDNA was amplified by PCR with pSRαRev [13] as the template and with the primers 5′-AAA AAA AGATCT ATG GCA GGA AGA-3′ (Rev-*Bgl*II) and 5′-AAA AAAGTCGAC CTA TTC TTT AGTT-3′ (Rev-*Sal*I). The PCR product was digested with *Bgl*II and *Sal*I and then cloned into pEGFP-C1 (BD Biosciences Clontech, Palo Alto, CA) or pcDNA4/HisMax-C that had been digested with *Bam*HI and *Xho*I; the resulting vectors were designated pEGFP-Rev or pcMax-Rev.

2.4. Luciferase, chloramphenicol acetyltransferase (CAT), and p24 enzyme-linked immunosorbent (ELISA) assays

HEK293T cells were cotransfected with HIV-1 proviral DNA (pNL43 [14], pNL-Luc-E^-R^+ [15], or pNL-enCAT [16]) and TTP expression vectors (pchTTPwt, pcD1–101, pcD76–189, or pcD176–320) with the use of Fugene 6 (Roche, Mannheim, Germany) or by the calcium phosphate method. The amount of virus in culture supernatants was quantified by measurement of p24 antigen with a p24 Gag antigen capture ELISA assay (ZeptoMetrix, Buffalo, NY). For measurement of luciferase activity or CAT [17], cells were lysed and assayed with a Luciferase Assay System (Promega, Madison, WI) and a Lumat LB 96V luminometer (Perkin Elmer) or with a CAT ELISA (Roche).

Expression of wild-type and mutant TTP was examined by immunoprecipitation, SDS–polyacrylamide gel electrophoresis and immunoblot with mouse monoclonal antibodies to the Xpress epitope (Invitrogen) analysis or goat polyclonal antibodies to TTP (Santa Cruz Biotechnology, Santa Cruz, CA). The antibodies to Nef and to p24 also used for immunoblot analysis were kind gifts from Dr. Ikuta. Signals were obtained

with the ECL detection system (Amersham Pharmacia) and digitized with an LAS1000 imaging system (Fujifilm, Tokyo, Japan).

2.5. RT–PCR and virus infection

Cellular total RNA or virion RNA was subjected to RT with a 15-nucleotide poly(dT) primer and the use of an Omniscript kit (Qiagen, Valencia, CA). The resulting cDNA was subjected to quantitative analysis with a real-time, 5′-exonuclease PCR-based assay (TaqMan) and primer–probe combinations that were selected with the use of Primer Express software (Applied Biosystems, Foster City, CA) as specific for the coding regions of the tat, env, or luciferase genes. The reaction was performed with a QuantiTect Probe PCR kit (Qiagen) and an amplification protocol comprising incubation at 95 °C for 15 min followed by 45 cycles of 95 °C for 15 s and 60 °C for 1 min. The primers 1459F (5′-GGT CCT ATG ATT ATG TCC GGT TATG-3′) and 1535R (5′-TGT AGC CAT CCA TCC TTG TCAA-3′), and the probe 1491P (5′-FAM-TCC GGA AGC GAC CAA CGC CTT-TAMRA-3′, in which FAM indicates 6-carboxyfluorescein and TAMRA indicates *N,N,N′,N′*-tetramethyl-6-carboxyrhodamine) were used for detection of luciferase cDNA; the primers 7484F (5′-ATA AAC ATG TGG CAG GAA GTA GGAA-3′) and 7572R (5′-AGC AGC CCA GTA ATA TTT GAT GAAC-3′), and the probe 7513P (5′-FAM-AAT GTA TGC CCC TCC CAT CAG TGG ACA-TAMRA-3′) were used for that of env cDNA; the primers 6016F (5′-CAG ACT CAT CAA GCT TCT CTA TCA AAG-3′) and 8465R (5′-CGT TCA CTA ATC GAA TGG ATC TGT-3′), and the probe 8392P (5′-FAM-ACC CGA CAG GCC CGA AGG AAT AGA A-TAMRA-3′) were used for that of rev, tat and nef cDNA; the primers 5918F (5′-GTT GCT TTC ATT GCC AAG TTTG-3′) and 6017R (5′-TGA CTG TTC TGA TGA GCT CTT CGT-3′), and the probe 5945P (5′-FAM-TGA CA A AAG CCT TAG GCA TCT CCT ATG GC-TAMRA-3′) were used for that of the second exon of tat; the primers TTP 405F (5′-GCT GCG CCA GGC CAA TC-3′) and TTP 477R (5′-GCA GCG GCC CTG GAG GTA-3′), and the probe TTP 423 (5′-FAM- CCA CCC CAA ATA CAA GAC GGA ACT CTG TC-3′) were used for that of TTP cDNA. The transcripts detected by the env region primers and probe include both unspliced (9 kb) and singly-spliced (4 kb) RNA molecules, whereas those detected by the tat, rev and nef cDNA primers and probe include multiply-spliced transcripts (2 kb) [15]. The RNA copy numbers of luciferase, HIV-1 transcripts and TTP were determined with pGL3-promoter, pNL-Luc-E^-R^+, pSRαRev and pchTTPwt as a standard, respectively.

Vesicular stomatitis virus envelope-glycoprotein (VSV-G)-pseudotyped HIV-1 was produced by cotransfection of pNL-Luc-E^-R^+ and the VSV-G expression vector pHIT/G [18] in HEK293T cells. VSV-G-pseudotyped NL-Luc virus was infected to HEK293T cells transfected with TTP-expression vector or an empty vector. Following exposure to actinomycin D, an inhibitor of transcription, the copy numbers of multiple spliced or un-, singly spliced transcripts were determined by RT–PCR.

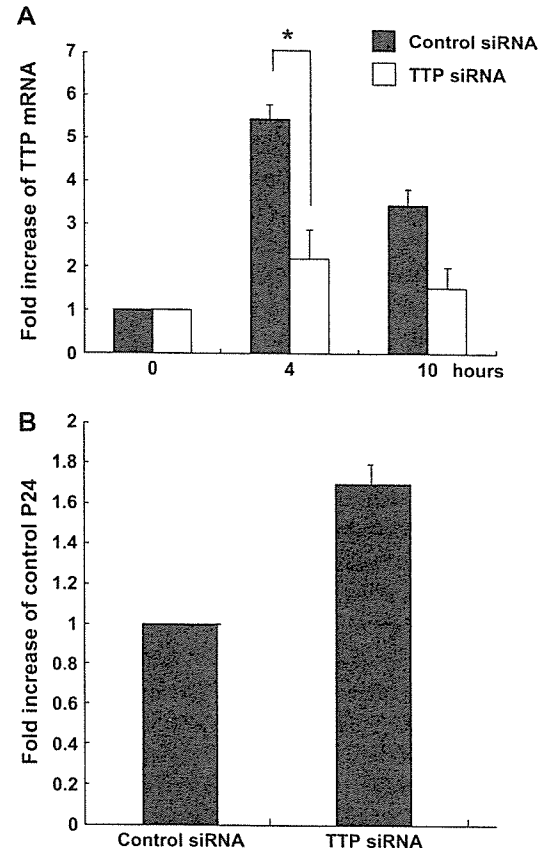

Fig. 1. Reduction of endogenous TTP increased HIV-1 production in U1 cells. (A) U1 cells were treated with two rounds of siRNA for TTP and controls. Following exposure to 7.5 ng/ml of PMA for 0, 4, or 10 h, the amount of TTP mRNAs were determined by RT–PCR and represented as the relative ratio against that of the cells before exposure to PMA. Data are means ± S.D. of values from three independent experiments. (B) Viral products (p24) of the supernatants of similarly treated cells as in (A) after 48 h post PMA stimulation were measured. $*P < 0.05$.

2.6. Preparation of RNA substrates

Substrate RNAs were prepared by in vitro transcription with T7 RNA polymerase and DNA amplified by the PCR as the template. DNA fragments that include the T7 promoter and encode RNA substrates of 75 and 93 nucleotides (nt) corresponding to the p7 and RRE were thus synthesized by PCR with the following primers: p7F (5′-TAA TAC GAC TCA CTA TAG GGA ACA AAT CCA GCT ACC ATA ATG ATA-3′) (underlining denotes T7 promoter) and P7R (5′-ATT GAA ACA CTT AAC AGT CTT-3′), corresponding to nt 1900 to 1971 of pNL43, GenBank accession number, M19921; stem II of RRE; U-GF (5′- AAA TAA TAC GAC TCA CTA TA GGGAG CAG CAG GAA GCA CTA TGG GCT-3′) and U-GR (5′-TTG TTC TGC TGC TGC ACT ATA TCA GAC AAT-3′), corresponding to nt 7783 to 7875. The RNA molecules were labeled at the 5′ end with [γ-^{32}P]ATP and

polynucleotide kinase after dephosphorylation with calf intestinal phosphatase. They were purified by electrophoresis on denaturing 15% polyacrylamide gels containing 7 M urea with the use of a Mini Whole Gel Eluter (Bio-Rad, Hercules, CA). The concentration of RNAs was determined by spectrophotometer (NanoDrop technology, Wilmington, DE).

2.7. Analysis of proteins and enzyme purification

Recombinant TTP protein was produced by overexpression in *Escherichia coli* using an His_6-tagged prokaryotic expression vector, pQE-9 (Qiagen) encoding TTP cDNA (GenBank accession number, M63625) [19]. Recombinant proteins were purified using an HiTrap chelating column (Amersham Pharmacia, Biotech, Freiburg, Germany) [20]. After staining with SYPRO (Molecular Probes), the polyacrylamide gel was visualized with FLA 2000 (Fujifilm).

2.8. Immunofluorescence analysis

HeLa cells were transfected with pEGFP-Rev and either pcDNA4/HisMax-C, pchTTPwt, pcD1–101, pcD76–189, or pcD176–320. After 24 h, the transfection mixture was removed and the cells were washed twice with phosphate-buffered saline (PBS), treated with 0.5% trypsin in 0.1 mM EDTA, suspended in culture medium, and plated on coverslips. The cells were then incubated for 2 h at 37 °C, fixed for 1 h at room temperature with 4% paraformaldehyde in PBS, and permeabilized for 5 min with 0.1% Triton X-100 in PBS. After quenching with 0.1 M NH_4Cl at room temperature for 10 min, the cells were incubated with 10% fetal bovine serum in PBS before consecutive exposures for 1 h at room temperature first to antibodies to the Xpress epitope in PBS containing 0.5% gelatin, 10 mM glycine, 10 mM EDTA, and 0.05% NaN_3 and then to Alexa Fluor 543-conjugated goat polyclonal antibodies to mouse immunoglobulin

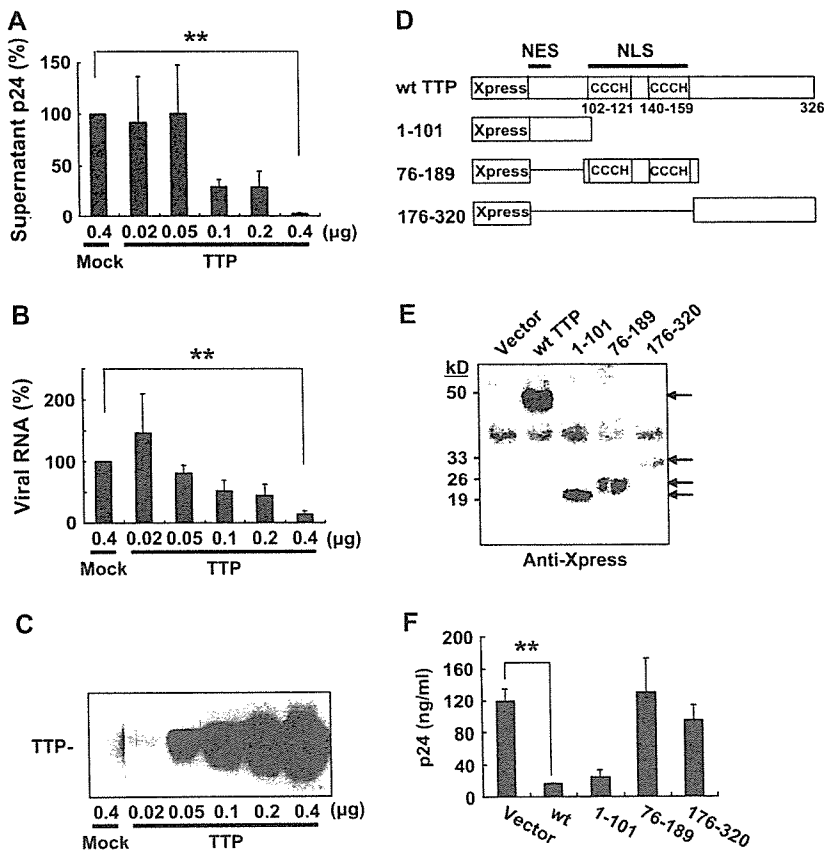

Fig. 2. Suppression of HIV-1 production by exogenous TTP. HEK293T cells (5×10^5 per well in a 12-well dish) were cotransfected with HIV-1 proviral DNA (0.04 μg of pNL-Luc-E^-R^+) and either the indicated amounts of an expression vector for TTP tagged with the Xpress epitope (pchTTPwt) or the corresponding empty vector (0.4 μg). The cells were subsequently cultured for 48 h in fresh medium, after which the amounts of p24 (A) and HIV-1 genomic RNA (the second exon of tat) (B) in the culture supernatants were determined; data are expressed as a percentage of the values for cells transfected with the empty expression vector and are means ± S.D. of values from three independent experiments. Cell lysates were also subjected to immunoblot analysis with an antibody to the Xpress epitope tag (C). $^{**}P < 0.02$. (D) Schematic representation of TTP mutants. Xpress tag, zinc finger domain (CCCH), nuclear export signal (NES), nuclear localization sequence (NLS) and the number of amino acid (326) are indicated. (E) Immunoprecipitation using an antibody to the Xpress epitope of the lysates from HEK293T cells expressing Xpress-tagged wild-type (wt) or mutant forms of TTP, followed by immunoblot analysis with the same antibody. (F) HEK293T cells (5×10^5) were cotransfected with pNL-Luc-E^-R^+(0.04 μg) and either an expression vector for wild-type or mutant TTP (0.4 μg) or the corresponding empty vector. The cells were subsequently cultured for 48 h in fresh medium, after which the amount of p24 in the culture supernatants was determined. Data are means ± S.D. of values from three independent experiments. $^{**}P < 0.02$.

G (Molecular Probes, Eugene, OR). Fluorescence signals were detected with a confocal laser-scanning microscope (LSM 410; Carl Zeiss, Oberkochen, Germany).

3. Results

3.1. Reduction of endogenous TTP mRNA levels increased HIV-1 production

We initially examined whether reduction of endogenous TTP in a latently HIV-1 infected cell line would increase HIV-1 production following stimulation. The U1 cell line is transcriptionally latent in terms of HIV-1 expression, and is activated by treatment with several reagents [21,22]. Under normal culture conditions, less than 5% of the cells continuously express HIV-1 antigens [22]. Stimulation of U1 cells with phorbol 12-myristate 13-acetate (PMA) significantly increased the population of HIV-1 antigen-expressing cells up to 40% at 10 h. At the present time, no antibody capable of detecting human endogenous TTP expression is available (personal communication). Therefore, we examined TTP mRNA levels in U1 cells transfected with TTP siRNA or control siRNA. Following treatment of PMA, TTP mRNA peaked at 4 h in U1 cells transfected with control siRNA (Fig. 1A), as previously reported [23]. In contrast, in U1 cells transfected with TTP siRNA PMA stimulation increased TTP mRNA significantly less than cells transfected with control siRNA. Following 48 h stimulation by PMA, p24 levels in the supernatant in U1 cells transfected with TTP siRNA were found to be increased (Fig. 1B), suggesting that TTP decreases HIV-1 production.

3.2. Suppression of HIV-1 production by exogenous TTP

To determine whether exogenous TTP is able to affect HIV-1 production, we co-expressed human TTP and the HIV-1 clone pNL-Luc-E$^-$R$^+$ [24] in HEK293T cells. The amounts of p24 and genomic RNA in culture supernatants were markedly reduced by TTP (maximal inhibition of 97% and 86%, respectively) in a concentration-dependent manner (Fig. 2A–C).

We investigated the functional domains of TTP responsible for the inhibition of HIV-1 production by co-expressing various TTP mutants (Fig. 2D,E) with pNL-Luc-E$^-$R$^+$ in HEK293T cells. A TTP mutant (1–101) that lacks the COOH-terminal region containing the nuclear localization sequence (NLS) inhibited HIV-1 virion production to an extent similar to that observed with the wild-type protein (Fig. 2F). In contrast, the NH_2-terminal deletion mutants 76–189 and 176–320, both of which lack the nuclear export sequence (NES), did not significantly inhibit HIV-1 production (Fig. 2F). The expression level of TTP mutant (176–320) was much lower than other recombinant wild-type and mutants TTPs (1–101 and 76–189) and this result was also observed when the mutants were subcloned into another plasmid, pcDNA4/HisMax-C used in the Fig. 6, suggesting the amino acid residue (1–175) might play a role in stable

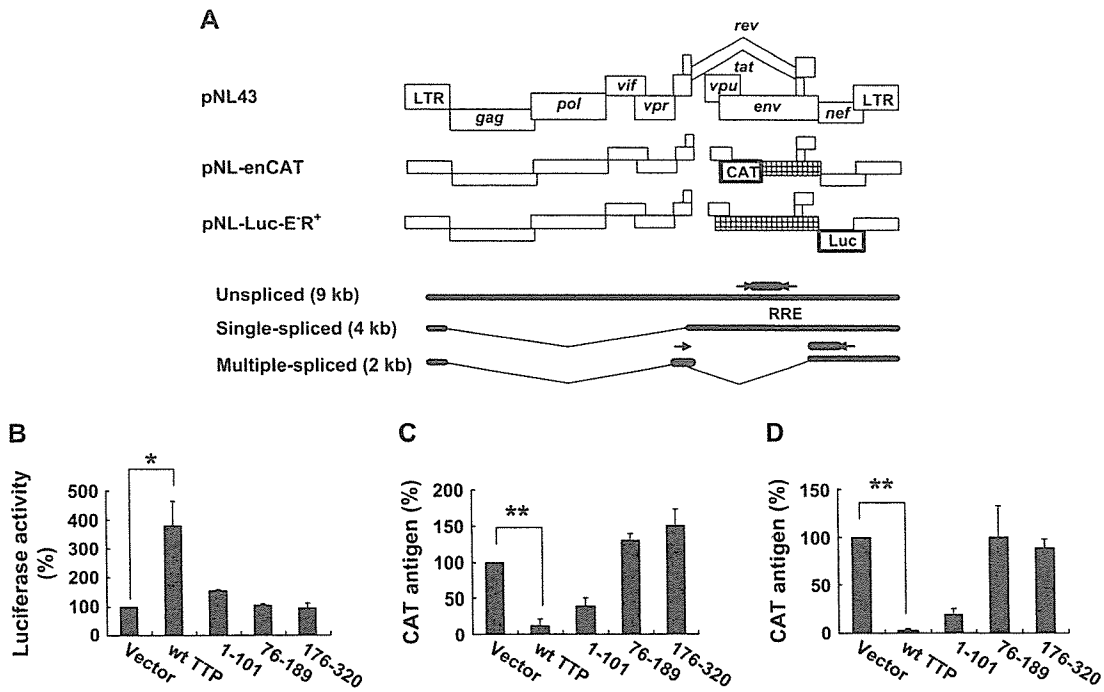

Fig. 3. Promotion of multiple splicing of HIV-1 RNA by TTP. (A) Schematic representations of pNL43, pNL-enCAT, and pNL-Luc-E$^-$R$^+$. The sites of PCR primers and probes for quantitative PCR were indicated as arrows. (B) HEK293T cells (5×10^5) were transfected with an expression vector for wild-type or mutant TTP (0.4 μg) and then infected for 48 h with VSV-G-pseudotyped NL-Luc virus (1 ng of p24) (B) or NL-enCAT virus (1 ng of p24) (C), after which the amounts of luciferase activity (B) or CAT antigen (C) in cell lysates were determined. Data are means ± S.D. of values from three independent experiments. (D) HEK293T cells were cotransfected with pNL-enCAT (0.04 μg) and an expression vector for wild-type or mutant TTP (0.4 μg), and the amount of cellular CAT antigen was determined after incubation for 48 h. Data are means ± S.D. of values from three independent experiments. *$P < 0.05$, **$P < 0.02$.

expression of the protein, because the expression plasmid of this mutant has the same promoter as those of other mutants.

3.3. TTP influences the production of un-, single- and multiple-spliced transcripts

To examine which steps of HIV-1 replication were influenced by TTP, we next used HIV-1 reporter viruses and distinguished viral products associated with un-, single- and multiply spliced transcripts (Fig. 3A). HEK293T cells were transfected with an expression vector for wild-type or mutant TTP and then infected with the pseudotyped NL-Luc virus. The luciferase activity of the cells was increased significantly (4-fold) by wild-type TTP and to a lesser extent (1.5-fold) by the 1–101 mutant, whereas the NH_2-terminal deletion mutants 76–189 and 176–320 did not affect the luciferase activity (Fig. 3B). We then examined the expression of CAT in cells either inoculated with the NL-enCAT pseudovirus containing the HIV-1 chimeric genome of pNL-enCAT (Fig. 3A,C) or transfected with pNL-enCAT (Fig. 3A,D), both of which contain the CAT reporter gene in place of the env open reading frame [15]. In both instances, the expression of CAT was markedly inhibited by wild-type TTP or the 1–101 mutant but not by the NH_2-terminal deletion mutants 76–189 or 176–320. These results indicated that TTP promoted multiple splicing of HIV-1 transcripts, thereby increasing the products of the 2-kb spliced RNA and decreasing that of unspliced (9 kb) and single-spliced (4 kb) RNAs. Although the 1–101 mutant decreased the expression of CAT, the mutant did not significantly affect on the luciferase activity, suggesting that the mechanism of suppression of CAT activity by wild-type and the 1–101 mutant TTP seemed to be different.

To confirm that TTP affects HIV-1 replication through regulation of splicing, we co-expressed TTP and the HIV-1 clone pNL43 in HEK293T cells and examined expression levels of

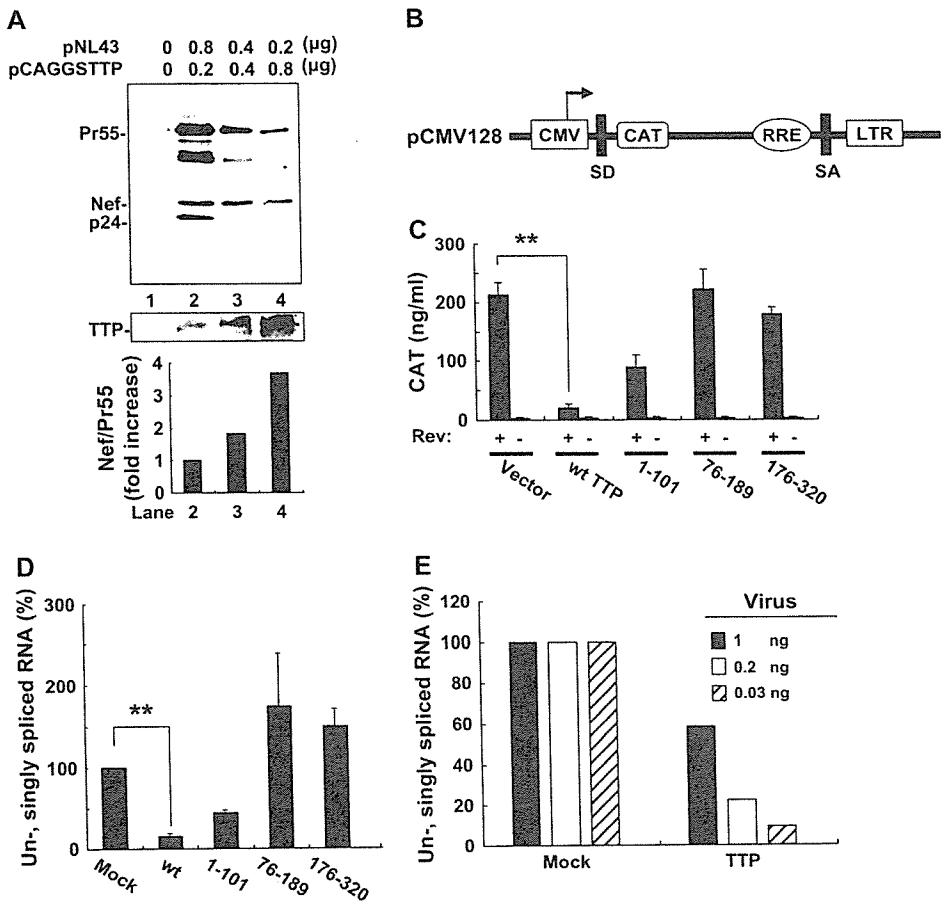

Fig. 4. Effects of TTP on HIV-1 RNA splicing. (A) HEK293T cells were cotransfected with the indicated amounts of pNL43 and of a TTP expression vector (pCAGGSTTP), after which cell lysates were subjected to immunoblot analysis with antibodies to p24 and to Nef (upper panel) or with those to TTP (lower panel). The Nef/$Pr55^{gag}$ signal ratio for the blot was determined and expressed as fold increase relative to the value for lane 2. (B) Schematic representation of the Rev reporter plasmid pCMV128. The CMV promoter (CMV), splice donor (SD), splicing acceptor (SA), and HIV-1 long terminal repeat (LTR) are indicated. (C) HEK293T cells were cotransfected with pCMV128 (0.1 μg) and an expression vector for wild-type or mutant TTP (0.4 μg) in the absence or presence of pcMax-Rev (0.4 μg). The cells were then incubated for 48 h in fresh medium before determination of the amount of intracellular CAT antigen. Data are means ± S.D. of values from three independent experiments. $^{**}P < 0.02$. (D) HEK293T cells were transfected as in (Fig. 3B) and the relative ratio of the number of un-, singly spliced transcripts (9 and 4 kb) to the number of those reactive with multiply-spliced transcripts (2 kb) was determined. Data are means ± S.D. of values from three independent experiments. (E) Cells transfected with pchTTPwt (0.4 μg) and then infected with VSV-G-pseudotyped NL-Luc virus (1, 0.2, or 0.03 ng of p24 antigen) were assayed for viral RNA splicing as in (A). Data are from a representative experiment. $^{**}P < 0.02$.

Gag and Nef proteins. Although the intracellular levels of Gag proteins (Pr55, p24) was substantially decreased by co-expression of TTP, those of Nef were not affected (Fig. 4A). The ratio of the amount of Nef to that of $Pr55^{gag}$ was found to be increased by TTP in a concentration-dependent manner (Fig. 4A). Furthermore, we investigated the effects of TTP with the use of different expression system, pCMV128, a Rev reporter plasmid that encodes most of the env sequence and a Rev-responsive element (RRE) downstream of the CAT gene, with splice donor and splice acceptor sites at the 5′ and 3′ ends of the construct, respectively [25] (Fig. 4B). Both wild-type TTP and the 1–101 mutant markedly suppressed CAT expression in HEK293T cells transfected with pCMV128 and a Rev expression plasmid, whereas the NH_2-terminal deletion mutants of TTP (76–189, 176–320) had no effect (Fig. 4C). These results thus indicated that TTP and its 1–101 mutant suppressed the Rev-induced gene expression.

3.4. Effects of TTP and its mutants on the splicing of HIV-1RNA

Because TTP decreased the products of the un-, single spliced transcripts of HIV-1 and increased multiple spliced transcripts, we examined the effects of TTP and its mutants on the splicing of HIV-1 RNA in cells transfected with pNL-Luc-E^-R^+ (Fig. 3A). Wild-type TTP induced significant decrease (86%) in the proportion of unspliced HIV-1 RNA (assessed from the ratio of the abundance of transcripts detected by the env probe to that of those detected by the tat, rev and nef cDNA probe) compared with the cells transfected with the corresponding mock vector (Fig. 4D). The TTP mutant 1–101 induced a smaller decrease (56%) in the proportion of unspliced HIV-1 RNA, whereas the NH_2-terminal deletion mutants (76–189 and 176–320) had no effect (Fig. 4D). Similar results were obtained with HEK293T cells inoculated with the VSV-G-pseudotyped NL-Luc virus (Fig. 4E). The proportion of unspliced HIV-1 RNA in cells infected with a low titer (0.03 ng of p24) of the pseudotyped NL-Luc virus was reduced by 10% by co-expression of TTP (Fig. 4E). These results thus suggested that TTP enhanced the multiple splicing of HIV-1 transcripts.

To examine whether TTP destabilizes HIV-1 RNA, we compared the effects of TTP on the RNA stability of wild-type HIV-1. However, TTP did not significantly affect the rate of RNA decay of both multiply spliced and un-, singly-spliced RNA for 180 min (data not shown).

3.5. TTP binds to HIV-1 AU-rich RNA

That AU residues of inhibitory sequence in of HIV-1 RNA can complement Rev activity [26] and replacement of AU residues of HIV-1 mRNA without alteration of the encoded proteins has been reported to result in marked expression of HIV-1 Gag, Pol, and Env proteins independent of the Rev/RRE/Crm1, suggesting that the AU-rich negative elements are necessary for the responsiveness of late HIV-1 transcripts to Rev [2,3]. As TTP binds to AU-rich elements [10], the P7 region, which has high ratio of AU residues (63%), was chosen in the HIV-1 sequence. Meanwhile, the RRE is known as a structural region bound to Rev and has relatively low AU sequence (48%). Therefore, as a control, we used a synthesized RNA of the RRE. To analyze the binding in an acrylamide gel we chose a stem loop region of the RRE, stem II, which is a minimal RNA element for Rev binding [27]. We synthesized both RNA of p7 and stem II of the RRE, which was found to contain small amount of longer substrates (Fig. 5B, black arrow). The binding assays revealed that TTP bound to P7 sequence (Fig. 5A) much more strongly than that of stem II of the RRE (Fig. 5B). To confirm that TTP specifically bound to the P7 sequence, we examined whether unlabeled P7 inhibited the binding of TTP. Unlabeled P7 RNA inhibited the binding of TTP to labeled P7 in a concentration-dependent manner, but stem II of the RRE did not (Fig. 5C).

3.6. Effects of TTP on the subcellular localization of Rev

To investigate the mechanism of suppression of HIV-1 replication by wild-type and 1–101 mutant TTP, Rev fused with

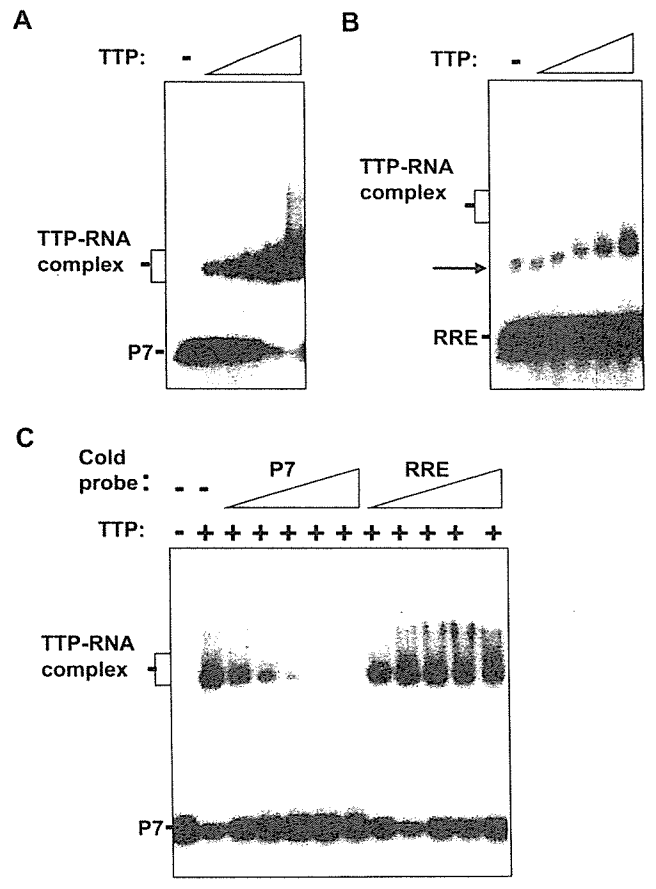

Fig. 5. Binding of TTP to the p7 RNA. Native electrophoretic mobility-shift assay of the binding of TTP (0.05, 0.1, 0.25, 0.5, or 1 μg/ml) to the ^{32}P-labeled P7 (A) or stem II of RRE (B) RNA (10 ng) in a final volume of 10 μl. Control reactions were performed in the absence of TTP(-). The positions of the free RNA molecule of P7 (75 nt), of RRE (93 nt) and of the TTP–RNA complex are indicated. (C) The binding of TTP (0.25 ng) to the ^{32}P-labeled P7 RNA (3 ng), which was mixed with different amounts of unlabeled P7 and unlabeled stem II of RRE RNA (0, 1.25, 2.5, 5, 10, and 20 ng in each lane).